A critical review on designs and applications of microalgae-based photobioreactors for pollutants treatment

Hoang Nhat Phong Vo[1], Huu Hao Ngo[1,*], Wenshan Guo[1], Thi Minh Hong Nguyen[2], Yiwen Liu[1], Yi Liu[3], Dinh Duc Nguyen[4], Soon Woong Chang[4,*]

[1] *Centre for Technology in Water and Wastewater, School of Civil and Environmental Engineering, University of Technology Sydney, Sydney, NWS 2007, Australia*
[2]*School of Environment, Resources and Development, Asian Institute of Technology, P.O. Box.4, Klong Luang, Pathumthani, 12120, Thailand*
[3]*Shanghai Advanced Research Institute, Chinese Academy of Science, Zhangjiang Hi-Tech Park, Pudong, Shanghai, China*
[4]*Department of Environmental Energy Engineering, Kyonggi University, 442-760, Republic of Korea*

***** Corresponding author: *E–mail address: *Corresponding authors: 1st corresponding author: H. H. Ngo; E–mail address: ngohuuhao121@gmail.com, and 2nd corresponding author: S. W. Chang, Email address: swchang@kyonggi.ac.kr*

Abstract

The development of the photobioreactors (PBs) is recently noticeable as cutting-edge technology while the correlation of PBs' engineered elements such as modellings, configurations, biomass yields, operating conditions and pollutants removal efficiency still remains complex and unclear. A systematic understanding of PBs is therefore essential. This critical review study are to: (1) describe the modelling approaches and differentiate the outcomes; (2) review and update the novel technical issues of PBs' types; (3) study microalgae growth and control determined by PBs types with comparison made; (4) progress and compare the efficiencies of contaminants removal given by PBs' types and (5) identify the future perspectives of PBs. It was found that Monod model's shortcoming in internal substrate utilization is well fixed by modified Droop model. The corroborated data also remarks an array of PBs' types consisting of flat plate, column, tubular, soft-frame and hybrid configuration in which soft-frame and hybrid are the latest versions with higher flexibility, performance and smaller foot-print. Flat plate PBs was observed with biomass yield being 5 to 20 times higher

than other PBs types whilst soft-frame and membrane PBs could also remove pharmaceutical and personal care products (PPCPs) up to 100%. Looking at an opportunity for PBs in sustainable development, the flat plate PBs are applicable in PB-based architectures and infrastructures indicating an encouraging revenue-raising potential.

Keywords: Microalgae; Photobioreactors; Pollutants Treatment; Modelling

Abbreviations

COD Chemical Oxygen Demand

DIP Dissolved Inorganic Phosphorus

DO Dissolved Oxygen

EVA Ethylene Vinyl Acetate

HRT Hydraulic Retention Time

LDPE Low Density Polyethylene

O&M Operation and Maintenance

PBs Photobioreactors

PE Polyethylene

PPCPs Pharmaceutical and Personal Care Products

PTFE Polytetrafluoroethylene

TN Total Nitrogen

TP Total Phosphorus

WCC-PBs Water-Circulating Column PBs

Notations

$\bar{\mu}$: average total specific growth rate, /h

μ_L: *volumetric growth rate, mg/L.d*

μ_x: algal growth rate, /d

μ_X: the algal specific growth rate, d^{-1}

μ_d: cell decay rate, L/h.g

ν_{Fe}: Fe uptake rate, g_{Fe}/g dry weight.min

ν_{Fe}^{max}: maximum Fe uptake rate, g_{Fe}/g dry weight.min

ρ: biomass growth kinetic, /d

$C_{Fe(III)}$: total mass concentration of Fe(III) in bulk phase, mg Fe/L

K_{Fe}: half saturation constant of Fe, mg Fe/L

q_{Fe}: Fe cell quota, g_{Fe}/g biomass

Q_{Fe}^{max}: maximum Fe cell quota which iron uptake is stopped, g_{Fe}/g biomass

Q_{Fe}^{min}: minimum Fe cell quota which growth is inhibited, g_{Fe}/g biomass

A and *B:* pre-exponential coefficients, /h

AC: Carbon assimilated by algae, mg/L

$Adsorb_{Me,ALGij}$: Adsorption of metal *j* to microalgae species *i*

ALG_i: microalgae concentration for species i

AN: Nitrogen assimilated by algae, mg/L

AP: Phosphorus assimilated by algae, mg/L

AR_j: metal-specific adsorption rate, h^{-1}

b: activation energy dependant constant

C: Cu concentration, mg/L

C_c: average carbon content, g carbon/ g dry cell weight

C_{cri}: critical Cu concentration, g/L

DIC: Dissolved Inorganic Carbon, mg/L

DIN: Dissolved Inorganic Nitrogen, mg/L

DIP: Dissolved Inorganic Phosphorus, mg/L

$E_{a,b}$: activation energy for cell growth, kJ/mol

I: local light intensity, μmol/m^2.s

I_i: Irradiance in reactor I, mol/m^2.d

K_C: inhibition constant, g/L

K_d*:* biomass loss rate, /d

K_i: Cu (II) inhibition constant, g/L

k_q*:* normalised minimum N quota for cell growth, unitless

k_s*:* light saturation terms for cell growth, μmol/m^2.s

K_S: Monod constant, g/L

m: empirical constant value

M_{CO2} and M_C: molecular weights of CO_2 and C

$MetalALG_{ij}$: Adsorbed metal complex for microalgae species *i*

$Metal_{F,j}$*:* Free-metal concentration for metal species and metal-microalgae complex *ji* (*i* = microalgae species, *j* = metal), μg/L

p: case-by-case value

P_i: internal substrate cell quota in reactor i

P_{min}: minimum biomass concentration, g/L

Q: influent volumetric flow rate, m^3/d

q: normalised N quota, unitless

r: NO_3^- uptake rate, mg/L.d

r_{max}: maximum NO_3^- uptake rate, mg/L.d

S_i: dissolved substrate concentration in reactor i, g/L

T: temperature, ^oC

TC: Total Carbon, mg/L

Th: biofilm thickness, μm

TN: Total Nitrogen, mg/L

TP: Total Phosphorus, mg/L

V_i: volume of PB number I, m^3

X: biomass concentration, g/L

X_i: biomass concentration in reactor number i, g/L

Y_C: yield coefficient for total carbon, (g_c g_x^{-1})

$Y_{N,P}$: N,P nutrient yield coefficient, (g_i $g_{biomass}^{-1}$)

1. Introduction

Algae are one of the most commonly known living organisms with multi-benefits received such as feedstock for biofuel production, tool of pollutant remediation and a rich source of pigment. For this reason, it has led to increasing demand for algae biomass in recent years. However, the natural environment (e.g. ponds, lakes) is unable to produce sufficient amounts of algae biomass. Therefore, man-made algae cultivation systems are being developed to expand the algae biomass yield. To this end, common algae cultivation systems can be classified as open and closed systems [1].

In the open systems, mono-algae culture is not fully secured. The purity of culture is difficult to control due to the invasion of other species. The operating conditions (e.g. pH, temperature, light intensity) fluctuate wildly and consequently, affect biomass yield [2-4]. For this reason, closed systems, like photobioreactors (PBs), are feasible options to tackle these drawbacks.

The first prototypes of PBs were initiated in the 1950s; later on, PBs were industrialized in food production. The application of PBs in pollutants treatment was begun at Carnegie Institute at Washington in 1953, employing in CO_2 sequestration [5]. PBs use robust and efficient algae cultivation techniques, and they create artificial environments which provide all essential conditions (e.g. light, temperature, nutrients and mixing) for algae growth. Those operating conditions are controlled and monitored [6]. PBs' designs and operations are particularly appropriate for microalgae cultivation. Microalgae growth is fast, constant and predictable. Currently, there are various types of microalgae-based PBs in terms of configurations, manufacturing materials and operation modes. The most common configurations for microalgae-based PBs are flat plate, column and tubular [1, 6, 7]. Later on, new versions namely soft-frame and hybrid PBs have been introduced and upgraded their flexibility and efficacies to higher level [8-10].

In this regard, each microalgae-based PB type has its own advantages and drawbacks, in terms of operation, biomass yield, pollutants removal efficiency and level of upscaling [11-13]. The configurations are renovated continuously to optimize biomass yield, improve efficiency in removing contaminants and reduce cost and space dominance [10, 14]. This has been shown in experiment works, coupling the validation of modelling softwares. The modelling approaches also apply multiple theories and principles which generate different outcomes [7, 15, 16]. Herein, the questions were raised about which types of PBs are preferred and what criteria are considered to compare these PBs. In addition, there is controversial whether or not PBs are suitable for pollutants treatment [5]. The future development and upscaling of PBs in a sustainable approach also gains much concern. Previously, there have been a number of review studies on microalgae-based PBs and they focused on the fragmental issues such as modelling [7, 17], biomass yield [3], PBs design [18, 19] and green development [20]. Thus, the nexus of PBs' configurations, modellings, biomass yields, relevant operating conditions and pollutants removal efficacies is unclear and it is re-organized in this study as in Fig. 1.

[Insert Figure 1]

Furthermore, some knowledge gaps related to microalgae-based PBs are highlighted as below:

- Different and conflicted results from PBs models are not clearly explained.
- The data of soft-frame and hybrid PBs has not been reviewed and verified with other PBs types.
- The efficiency of microalgae cultivation and control defined by PBs types are not well compared and interpreted.
- Lack of comparison amongst PBs types in terms of pollutants removal efficiency while PPCPs removal's knowledge is not progressed adequately.
- The collocation of PBs and building in sustainable concept are not up-to-date.

Thus, a good systematic understanding of PBs is essential to be made for elucidatting the mentioned knowledge gaps. More to the points, the corresponded objectives of this paper are to: (1) describe the modelling approaches and differentiate the outcomes; (2) review and update the novel technical issues of PBs' types; (3) study microalgae growth and control of different PBs; (4) examine and compare the efficiencies of contaminants removal given by PBs' types; and (5) progress the future perspectives of PBs.

2. Advances in photobioreactors' modelling

Microalgae-based PBs consist of multi-complicated biochemical processes (Fig. 2) in which photosynthesis and respiration are the two decisive ones. These processes establish a strong background for constructing any models. Algae cells in the models are comply to some assumptions including: (i) biomass with formula of $C_{106}H_{263}O_{110}N_{16}P$, (ii) inorganic carbon, (iii) inorganic nitrogen, (iv) oxygen and (v) chlorophyll [21]. In PBs' bulk liquid, the inorganic N and P, dissolved inorganic C and dissolved organic C were involved as critical nutrients sources with additional presence of heavy metals and pharmaceutical and personal care products (PPCPs). The effect of environmental factors such as light intensity and temperature is also important to microalgae-based PBs' modelling works. Thus, this section reviews the microalgae growth and pollutants removal dynamic with reference to the mentioned factors.

[Insert Figure 2]

2.1 Modelling of microalgae growth dynamic

The high microalgae growth dynamics and biomass yield in PBs are basic and fundamental expected outcomes. Many researchers have been attempting to control these matters via modelling, however, a variety of approaches has been employed [7]. A couple of models have been translated from theoretical processes in Fig. 2 to stimulate the microalgae growth dynamic.

To begin with, Monod model is a classical method used for estimating microorganism growth, including microalgae. For instance, Lee et al. [22] composed a guideline to maximize biomass productivity for outdoor PBs (e.g. open pond, vertical flat plate and horizontal tubular types) via the Monod model (Eq. 1). The biomass productivity corresponded to the ratio of initial microalgae concentration (X_o) and illuminated the surface area per unit volume (a). This delivered an optimal biomass yield of 0.045 kg/m^2.d at X_o/a = 0.035 kg/m^2 [22]. Noticeably, the experimental data and simulation well confirmed the results in both analyses [15, 22]. Al Ketife et al. [15] employed a modified Monod model (Eq. 2) for assessing the effect of initial nutrient concentration on biomass yield of *Chlorella vulgaris*. However, Al Ketife et al. [15] admitted that a better understanding was required with reference to operating conditions, reactor configurations, algal trains and scale-up. Meanwhile, Lee et al. [22] confirmed their outcomes complied with various micro-organism species and PB types.

Subsequently, Zhang et al. [16] applied the Droop model (Eq. 3) and the Luedeking–Piret model (Eq. 4), and concluded that the attached cultivation process achieved more biomass yield than suspended one. This finding was based on higher light attenuation of the suspended process due to microalgae absorption. The illumination in the suspended process reduced 71% and affected half of the reactor [16]. For the attached cultivation process, biofilm formation on media was considered an indicator for microalgae biomass development. The produced biomass was observed as creating a layer on media; however, there is no in-depth and quantitative study being conducted. Thus, the biofilm thickness of the attached growing process was later on simulated by Das et al. [23] (Eq. 5). From the basic self-deprived model, it was further developed to be applicable in both continuously operating circular and rectangular flat plate PBs [23]. The biofilm thickness ranged from 11.52 to 55.7 μm coupling malic acid concentration of 1 to 10 g/L as nutrient and its thickness became stable after 40 h if no nutrient replenish was given accordingly [23].

In large-scale application, microalgae biomass in series PBs was modelled via modified Droop model [24]. In detail, it was involved the biomass' internal substrate consumption and, thus, fitted in the series-type PBs' simulation (Eq. 6) [24]. Likewise, *PhotoBioLib* - a data library in *Modelica* software - was also managed by Perez-Castro et al. [25] to simulate large-scale PBs. The calculation methods of biomass yield are summarized in Table 1.

[Insert Table 1]

Generally, these modellings were observed at their own levels of accuracy and they were improved continuously for a higher scientific demand. It can be seen that Monod kinetic was the most traditional method, relying on average growth rate only. From its original form, there were a couple of modified versions being introduced. For example, the biomass loss rate was considered in the calculation of Eq. 2, improving its certainty to a higher step. On the other hand, the maximum specific growth rate (μ_{max}) of Monod model was also considered as a function of environmental factors (e.g., temperature and light intensity) in Eq. 7 [26]. Nevertheless, Monod model possessed a shortcoming whilst it only matched with proportional relationship of nutrients uptake and microalgae growth. Likewise, Monod model was reported to be failed elsewhere since it ignored the stored nutrients in microalgae cells [27]. The Droop model and Luedeking–Piret model involved temperature, light intensity and nutrient concentration additionally (Fig. 3). In the case that nutrients were completely consumed but algae biomass yield still enhanced extensively known as internal substrate consumption and it was failed with Monod model, modified Droop model could give a proper assist and fixed it [21].

[Insert Figure 3]

Apart from the biomass yield model, the photosynthesis process of microalgae was also studied in-depth. García-Camacho et al. [28] improved the mechanistic model of microalgae

photosynthesis considering photoacclimation dynamics compared to their own previous version [29] that based on the Michaelis-Menten formular of enzyme formation. In details, the disappearance rate, photoinhibition and damaged repair of photosynthetic units were included extensively. Brindley et al. [30] confirmed the accuracy of the photosynthesis dynamic model proposed by García-Camacho et al. [28].

The influence of illumination patterns in PBs has increasingly attracted researchers' interest. Light is a key factor determining biomass yield and consequently, optimizing light received by microalgae is a challenging task. Murphy and Berberoğlu [31] examined the photosynthetic rate of microalgae species (e.g. *Chlamydomonas reinhardtii* and *tla1*) via modelling tools. The empirical model was firstly constructed from experimental data to achieve a specific photosynthetic rate under local irradiance. Subsequently, the prediction of local and total photosynthetic rates, applying radiative transfer equation, was undertaken. The outcome reported that sunlight irradiance of 400 W/m^2 could increase biomass productivity by approximately 30% [31]. Kong and Vigil [32] insisted that one dimensional model could not calculate light intensity distribution. Therefore, two and three dimensional models, based on Mie theory, were built to observe light scattering and absorption by microalgae. Furthermore, light is known to generate heat and encourage microalgae growth. Jiménez-González et al. [33] analyzed heat balance in the inner illumination PBs by applying the grey-box model. However, this model may have to deal with noise disturbance [33]. Fuente et al. [34] successfully emulated light attenuation for industrial-scale application. The wild type and olive strains of *Synechocytis* sp. PCC 6803 were used in flat plate PBs under red, white, blue and green LED light. LED offered polychromatic light source, compared to monochromatic one of fluorescent light [34]. Although this was conducted in flat plate PBs, it could be adjusted to suit any types of PBs, illumination spectrums and designs [34].

Regarding the hydrodynamic conditions, they were employed to assess microalgae growth in multiple approaches. Marshall and Sala [35] used the stochastic Lagrangian model to predict microalgae growth via turbulence mode. Microalgae growth was found to increase with Reynolds number but it was subsequently stable beyond the Reynolds number threshold of 9×10^4 [35]. The difference between the experimental data and computational calculation was 10% [35]. Furthermore, the calculated biomass yield by the Eulerian model was less than that managed by the Lagrangian method [36]. However, the Lagrangian model remained the limit in particles tracking, so that the discrepancy between experiment and simulation results happened [36]. Besides, the nutrient limit occurring in the experiments, but it was not considered in simulation works, was another cause of the different results [36].

Fernández et al. [37] predicted the impact of biomass yield would result in a changing pH gradient, dissolved oxygen (DO), photosynthesis rate and dissolved CO_2 in tubular TBs. For example, the photosynthesis rate was maximized corresponding to biomass yield from 0.2 to 2 g/L thanks to the insignificant mutual shading effect of microalgae cells [37]. This result is highly applicable in practice. Similarly, this model could be modified for modelling other types of PBs [37]. More comprehensively, Shriwastav et al. [38] completed a microalgae-growth-predicting model with 37 parameters. Their work extends to the synergistic effect of bacteria and microalgae in PBs.

Some researchers understand the difference between the laboratory and natural environments as these can lead to variations in biomass yield results. Hence, it is important to tackle this issue. Lucker et al. [39] revealed the drawbacks of the ideally cultivated environments in laboratories which ignored microalgae species' biological responses to real environmental conditions. Consequently, the growth dynamics of microalgae were underestimated. The environmental PBs simulated real illumination patterns, which directly corresponds to water depth and other key factors (e.g. light, temperature, CO_2, nutrient, oxygen and mixing) [39].

Huesemann et al. [40] also simulated an outdoor open pond employing laboratory PBs to measure biomass productivity. There is a noticeable difference between laboratory and outdoor environments when it comes to biomass analysis methods, mixing conditions and light source (LED light in laboratory and sunlight in the outdoor context). For instance, the biomass productivity of *Chlorella sorokiniana* was lower 6.6 to 11.3% compared to outdoor conditions; however, it is higher 9.2% in the case of *Nannochloropsis salina* [40].

Overall, these modelling researches focus on estimating biomass yield, studying the effect of illumination patterns and temperature. Succinctly, some remarks are drawn as follow:

- Any biomass yield estimations are recommended to include two important parameters, encompassing temperature and light intensity.
- Specifically, whether suspended or attached the cultivation process attained a higher biomass yield but still proved to be controversial. It is likely suspended process received less illumination due to mutual shading effect of microalgae cells.
- There is also a significant difference between the laboratory and natural environmental conditions, resulting in variations or deviations in calculated biomass yield. Practically, the modelling results advised that biomass concentration being from 0.2 to 2 g/L received more advances in the operation processes.
- The shortcomings of Monod model possesses in temperature, light intensity and internal substrate utilization by microalgae have been curtailed by the Droop, Luedeking–Piret and modified Droop models.
- The increase of microalgae biomass yield was strongly determined by photosynthesis efficiency. More to the point, to have the photosynthesis process accurately simulated, the disappearance rate, photoinhibition and damaged repair of photosynthetic units should be included in the models.

2.2 Modelling of pollutant removal dynamics

Besides the microalgae growth dynamics, Shriwastav et al. [21] further modelled C, N and P assimilation in PBs (Eq. 8-10). Their research adopted three concepts, namely: general, biological-focusing coupling previous literature and biological-focusing without literature. Light intensity and temperature were the most important operational parameters. Accordingly, an increase in temperature of 10ºC had more effect, in terms of both biomass yield and pollutants removal efficiency, than enhancing light intensity of 10 times [21]. Nevertheless, each microalga has a different optimal temperature range. For example, *Fucus vesiculosus* suffered from severe effects of high temperatures (above 26ºC) [41], whereas *Chaetomorpha* sp. could survive with temperatures between 20.1 - 40.9°C [42]. This study processed with only *C. vulgaris* and *C. reinhardtii* and temperature was from 20 to 30ºC [21]. Thus, the comprehensive data of optimal temperature range should be constructed to prevent improper operation and control of microalgae in PBs that would render low pollutants removal efficiency. With regard to pollutant removal, the outcomes of P removal modelling received a notice given that the dissolved inorganic phosphorus (DIP) was almost unchanged at 15 mg/L after 5 d [21]. It is likely that microalgae-based PBs removed P inefficiently. This model was constructed with maximum P uptake rate of 0.08 mg P/mg biomass.d [21]. In a latter study, the addition of bacteria in microalgae-based PBs could enhance P removal efficiency to 100% of initial concentration of 6.53 mg/L in 3 d [38]. The applied maximum P uptake rate of bacteria in the updated model was 0.4 mg P/mg biomass.d which was five-fold higher than microalgae uptake rate [38]. Hence it was seen that the P assimilation was significantly contributed by bacterial consortium. The capability of N assimilation by algae and bacterial were quite similar with 0.6 and 0.9 mg N/mg biomass.d [38]. This outcome was useful for the treatment of high-P-concentration wastewater in which the PBs could be managed in such a way that bacteria community to be dominant. However, this PB was advised to operate with the balance of

bacteria and microalgae concentrations in PBs to maintain proper DO levels [38]. The dominance of bacteria community would reduce DO concentration and convert the system to anaerobic process [38]. Thus, in compliance with extensive simulation, the wastewater sources with low BOD_5 level and high nutrient concentration were recommended for this bacteria-microalgae concept provided that the effluent of secondary treatment of sewage wastewater was an alternative option [38].

In another study, Al Ketife et al. [15] programmed C, N, P removal efficiency (Eq. 11&12). The C source was from CO_2 while it was from dissolved organic compounds and CO_2 in the study of Shriwastav et al. [21]. Compared to Shriwastav et al. [21], the P removal dynamic was significantly higher in which microalgae could eliminate 90% of initial concentration of 4 to 6 mg P/L within 10 d. This can be explained by higher biomass concentration of 200-500 mg/L whilst Shriwastav et al. [21] achieved biomass yield less than 120 mg/L. Furthermore, the P yield efficiency in this study was 2.4 mg/g biomass that indicated a more dynamic assimilation rate of microalgae [15]. Notably, both studies built up the model with similar microalgae of *C. vulgaris* [15, 21].

With reference to CO_2 biofixation, the most common model was as in Eq. 13 and widely used by many authors [43-45]. It can be seen that CO_2 fixation rate in this model was proportional to the volumetric growth rate of microalgae and it was also dependable on the chosen C_c parameter's value (carbon content) amongst authors. For instance, Singh Khichi et al. [43] simulated the model with C_c of 0.63 g C/g biomass, whereas it was gone through of 0.48 g C/g biomass by Vo et al. [45] and Jacob-Lopes et al. [44]. Later on, this model was exploited in-depth by considering the correlation of carbonate chemistry and microalgae photosynthesis (Eq. 14) [46]. Critically, the author divided photosynthesis activity into three sections per day (morning, afternoon and evening) adapting to the different photosynthesis rates happened per

section [46]. This model also engaged the influence of pH and DO which was not in the previous one. Nevertheless, the author pinpointed the drawback of this model in which the assumption on photosynthesis rate was made once it was a function of inorganic carbon concentration; however, it was also potentially affected by cell density and light attenuation [46]. Alternatively, this could be handled by insightfully incorporating the relationship of light intensity and photosynthesis. Thus, this model would be useful in large-scale application. This model also applied to *C vulgaris* only but it built a strong background for extensively involving other microalgae species. More to the point, the model was constructed on per physical and chemical processes rather than the characteristic of microalgae so as the application to other microalgae types would be possible.

For the modelling of heavy metal assimilation in microalgae-based PBs, it has been reported by some authors given that these works are still limited in literature [27, 47, 48]. Typically, Concas et al. [27] developed an empirical formula to estimate Fe uptake rate by microalgae from Liebig's law (Eq. 15). This model well described the driven dynamic between internal iron concentration in microalgae cell and surrounded environment. According to the model, the internal iron source (0.0018 g Fe/g biomass) could help microalgae biomass survived and developed to 320 mg/L after 20 d even if no external Fe was supplied [27]. Similarly, the extended simulation was done by Richards and Mullins [49] who comprehensively studied the consumption of Fe, Mn, Ba, Ce, La by four types of microalgae encompassing *Nanochloropsis*, *Pavlova lutheri*, *Tetraselmis chuii* and *Chaetoceros muelleri* (Eq. 16). Unlike Concas et al. [27] who relied on previous theory, this study was a self-calibrated model. However, the remaining drawback was that none of these above models clearly addressed and quantified heavy metals adsorption and assimilation by microalgae-based PBs.

It is well known that N can be substantially consumed by microalgae as a vital source for cell built up. Amongst sources of N, NH_4^+ is assimilated preferably than NO_3^- because redox reaction will not happened with NH_4^+; thus, energy for biochemical reaction is reserved [50]. The consumption of these N sources was stated to be interfered by presence of metal ions [48]. Three bio-kinetic models were operated to evaluate the effect of Cu (II) on the NO_3^- utilization, consisting of modified Han-Levenspiel (Eq. 17), non-competitive inhibition (Eq. 18) and Andrews model (Eq. 19) [48]. Consequently, *Nostoc muscorum* was concluded as a promising microalgae for Cu removal with presented concentration up to 30 mg/L [48].

The summaries of pollutants assimilation models are illustrated in Table 2.

[Insert Table 2]

To this end, the following notices are highlighted related to the modellings of pollutants removal in PBs:

- The efficacies of P removal in PBs were still conflicted amongst authors. The different P consumption rates of applied algae between models were a reason.
- Lack of modelling researches at large-scale level and other pollutants assimilation (e.g., heavy metal and PPCPs).
- The validation of practical experiments and simulations may happen potential deviation. In the experimental part, the authors calculated the removal efficiencies through the differences of pollutants' concentrations in the influent and effluent of the bulk liquid. Most of the cases, the control experiments were missing. The quantification of pollutants assimilation by microalgae was important since other processes, such as adsorption, precipitation, hydrolysis and photolysis, might involve in the overall removal efficacies. On the other hand, the modelling method was established based on the pollutants assimilation kinetics by microalgae. Thus, the discrepancy of two platforms between practical experiments and

modelling works overestimated the actual capacity of microalgae. To tackle this, we recommend the experimental works should directly hand on the quantification of pollutants accumulation in microalgae cell. This can be conducted by using X-ray Powder Diffraction, Energy-dispersive X-ray for the case of C, N and P; or applying Solid Phase Extraction for heavy metals and PPCPs.

3. Advances in photobioreactors' designs and pollutants removal applications

In this section, the novel design approaches and process optimization techniques of PBs are described. The most popular types include tubular, flat plate, column and soft-frame PBs and some modified, hybrid systems (Fig. 4). Additionally, the efficiencies of microalgae growth and pollutants removal, being benefited from these novel designs and optimizations, are reviewed.

[Insert Figure 4]

3.1 Flat plate photobioreactors

Flat plate PBs consist of flat surface media which microalgae can attach to and develop. These types of PBs have many distinct advantages determined by the highly illuminated surface:volume ratio [51, 52]. A flat plate PB has minimal mechanical requirements and consumes not much energy [2, 53]. Also, increased biomass yield is achieved while the problems of biomass clogging, sedimentation or leakage are curtailed [6]. The effort to improve flat plate PBs' performance has been conducted over many years.

3.1.1 Innovations of configurations and operations

Regarding the modifications of configurations, Jung et al. [51] suggested the ultra-compact PBs to tackle unequal light distribution by using the stacked layers of slab waveguides with embedded light scatterers. The cultivation efficiency of 10-layer flat plate PBs was enhanced and biomass productivity improved 8-fold [51]. Similarly, the twin-layer porous sheet was

applied to augment biomass yield [54]. The porous between two layers allowed microalgae growth and minimized the detachment of microalgae to cultured media [54]. The isolated microalgae biomass also received more illumination and less opportunity exposing to unexpected contaminants and bacteria [54]. Ozkan et al. [55] also developed a biofilm attached surface by a 8 mm thick concrete layer lying on a wood supported plate and the designed cultivation area was 0.275 m^2. In another study, Sun et al. [52] integrated hollow polymethyl methacrylate tubes in flat plate PBs. The aluminum-coated polyethylene terephthalate was covered inner the tubes, aiming at forwarding the light transmittance to the dead zone of reactor, and doing so improved illumination in the interior zone by 2-6.5 times and biomass yield by 23.42% [52]. Likewise, Sforza et al. [56] enhanced photoconversion efficiency via photovoltaic panels in flat plate PBs given that the photovoltaic panels were placed in the middle of the reactor.

The local conditions also exerted an influence on flat plate PBs' performance. There are matrices of operating conditions in flat plate PBs (e.g. light path, panel orientation, panel distance, microalgae species, temperature), and the process of optimization is conducted to maximize biomass yield and reduce energy consumption. As such, Slegers et al. [57] proved that shade existing between panels had a negative effect which in turn reduced the penetration of light. The ideal distance between panels was 0.2 to 0.4 m [57]. Also, the north-south panel orientations produced 50% higher biomass yield than east-west orientation, especially in the high latitudes areas [57].

For operating conditions, Sierra et al. [2] examined the correlation of dissolved gas, heat transfer, mass transfer and mixing to aeration rates in flat plate PBs. The power supply of DO equipment was 53 W/m^3 which was similar to the bubble column PBs and less than the tubular unit of 2000-3000 W/m^3 [2]. Mixing time was less than 200 seconds which was 60 seconds

faster than bubble column PBs, and from 1 to 10 hours in the tubular PBs [2]. However, research implied the drawback increased the possibility of microalgae cells damage by aeration. Guo et al. [53] studied the effect of superficial gas velocity, top clearance on gas holdup liquid circulation speed, mixing time and mass transfer efficiency in airlift loop PBs. Consequently, the energy consumption was saved 16.3% [53]. Furthermore, the empirical model evidence suggested control and upscaling of the reactors. de Mooij et al. [58] proposed minimizing light absorption because over-illumination was unnecessary for generating biochemical energy. Thus, different light spectra in the form of various light colours were applied. The warm white and yellow light were witnessed the highest productivity which apparently doubled the productivity of blue light colour [58].

Not only were hands-on experimental studies undertaken; appropriate software was applied to support the research efforts. For example, Massart et al. [59] applied the Computational Fluid Dynamics model in flat panel airlift PBs to estimate optimal flowrate and maximize biomass yield. Firstly, the configuration of the PBs was calculated by Gambit® software; subsequently, simulation of the flow regime was carried out utilizing Fluent® software [59]. The optimal air flowrate was 1.5 L/min while mixing time was 312 s [59].

3.1.2 Microalgae growth and control

In a previously-reported microalgae biofilm PB, Ozkan et al. [55] progressed that *Botryococcus braunii* could generate significant biomass concentration, biomass productivity and lipid content of 96.4 kg/m^3, 0.71 $g/m^2.d$ and 26.8%, respectively. This biomass yield value was 35 times higher the any previous values in literature according to the authors [55]. Employing different microalgae strain, Koller et al. [60] concluded the *Scenedesmus ovalternus* growth reached its peak at 30ºC, pH 8.0 and photo flux of 1300 µmol photons/m^2.s in flat plate gas-lift PBs. The maximum biomass and growth rates were 7.5 ± 0.1 g/L and 0.11/h, respectively [60].

Given that illumination pattern possessed certain effect on biomass yield, the yellow light was explored producing the highest biomass yield (54 g/m^2.d) while blue and red light achieved almost half (29 g/m^2.d) [58]. Elsewhere, Pfaffinger et al. [61] increased biomass productivity of *Nannochloropsis salina* and *Nannochloropsis gaditana* up to 10.4 and 14.8 g/m^2.d, respectively, by optimizing LED illumination intensity. Finally, the adjustment of flow regime maximized biomass productivity at 87 mg/L.d [59].

Besides, biogas (e.g. ethylene) was a promising product which was constantly produced in stacked layers flat plate PBs (0.069 mg/L.h to 0.244 mg/L.h) [51]. This productivity was two times higher than the conventional flat plate PBs [51].

3.1.3 Pollutants removal

Through the Twin-layer PBs, Shi et al. [54] reported that N and P were removed 70-99%, which being 3 and 2 times, respectively, higher than the open pond system of Boelee et al. [62], in terms of uptake rates. The concentrations of N and P in the effluent were below 1.3 and 1 mg/L, respectively, and pleased the discharged standard of European Water Framework Directive. In another study, the maximum N and P uptake rates were 1.0 and 0.13 g/m^2.d, respectively [63]. This result, which used traditional biofilm reactor, was also lower than the Twin-layer PBs' one. Regarding CO_2 removal, Martín-Girela et al. [64] enhanced CO_2 adsorption up to 0.125 μmol CO_2/μmol photons in flat plate PBs.

3.2 Column photobioreactors

Column PBs are constructed in vertical column configuration. The culture is aerated by air or CO_2 gas for mixing, and to generate the suspended process. This type of PB has sufficient gas-liquid mass transfer, biomass yield and light/dark cycle control features [2, 33, 65-67]. The configuration of column PBs is simple in that they are designed by connecting modules and or combined with other techniques, especially the membrane process [68].

3.2.1 Innovations of configurations and operations

Provided that the change of PBs' configuration could optimize the operating conditions, Pham et al. [65] constructed column PBs in different shapes, including X-shape, H-shape and serial column, to improve hydrodynamic fluid and gas liquid mass transfer coefficient. The X-shape PB proved to be the best option, in terms of mixing time, gas liquid mass transfer coefficient, shear stress and flow rate [65]. Its mixing time was 23s compared to 1215s of serial column PB, whereas their gas-liquid mass transfer co-efficiencies were similar around 0.74 – 0.76 s^{-1} [65]. The X-shape PB encouraged the hydrodynamic conditions via its downcomer in the middle column, coupling the lowest shear stress [65]. Similarly, Janoska et al. [66] initiated the cultivation of microalgae in liquid foam to reduce harvesting and energy costs. Higher mass transfer and a drop in pressure in the foam-bed PBs were noticeable [66]. However, the liquid foam-bed can diminish illumination efficiency [66]. The current protein-based foaming agent (Bovine Serum Albumin) performed promisingly at the operation time of 8 h; nevertheless, the long-term operation required more stable agents [66].

In a broader context, Eltayeb et al. [69] proposed "Emerald Forest" microalgae-based PBs in a large-scale operation, with a consideration of the energy crisis, climate change and affordable housing. This was integrated with other technologies (e.g. wind farms, solar farms and power plants) to promote sustainable communities. The seawater, solar radiation and CO_2 from industrial activities were applied to microalgae cultivation. The PBs were designed to be shaped like trees, the aim being to maximize volume usage, illuminate surface area and decorate the landscape.

The illumination patterns and the light source position in column PBs are also considered to be attractive alternative options. Not only adopting the examined effects of illumination intensity [70], light was preferable when it was supplied from the internal zone [33, 67, 71, 72]. Hu and

Sato [67] optimized internal illumination by proper arrangement of blue and red LED light. The experimental data and modelling responded well. The distance of LED sources ranged from 30 to 50 mm while the illumination irradiance could be 250, 420 and 1000 μmol/m^2.s [67]. Importantly, the distance between LED sources was controlled and determined the biomass yield. Murray et al. [71] applied the internal illumination in the form of a free-floating wireless light source in submerged-light PBs. Subsequently, it achieved a biomass yield five-fold larger than external illumination [71]. The internal illumination alleviated negative effects of the dark zone and shade formation [71]. Pegallapati et al. [72] also achieved energy consumption six times lower than literature, when looking at and proposing internal illumination. López-Rosales et al. [73] scaled up bubble column PBs. The biomass yield was equivalent to laboratory-scale work while pH, temperature and air flow rate were maintained at 8.5, 21 ± 1ºC and 1.9×10^{-3} m/s, respectively [73]. This is the very first upscaling of bubble column PB to 80 L, equipped with LED. Ozkan and Rorrer [70] investigated the effect of light distribution on lipid and chitin nanofiber formation. Under the linear (70 μE/m^2.s) and saturation (370 μE/m^2.s) lighting concepts, lipid production was directly proportional to silicon uptake, coupled with the increase of biomass being achieved and corresponding to the increase in light intensity [70].

Besides, operating conditions (e.g. temperature, mixing) are important in column PBs. Serra-Maia et al. [74] confirmed temperature ranging from 18 to 25ºC did not seriously affect specific growth rate but a temperature above 25ºC did. The concept was applicable to chlorophyll pigment generation. Yang et al. [75] improved solution velocity in water-circulating column PBs (WCC-PBs) by water pump, the purpose being to reduce the use of energy. This decreased bubble generation time (31.1%) and mixing time (0.4%) occurred through the reduction of aerator and solution surface [75]. Compared to air-lifting column PBs, the WCC-PBs saved 21% energy consumption; however, biomass growth rate also fell by 12.7% [75]. Cheirsilp et

al. [76] applied repeated batch mode method in fluidized bed PBs which enhanced biomass and lipid production 2.66-fold and 1.41-fold, respectively. This suggests that operation cost could be reduced since no re-preparation process was required.

3.2.2 Microalgae growth and control

Lipid in microalgae is a desired product of the cultivation process. Hence, a number of related researches have been done to optimize lipid yield. For example, Ozkan and Rorrer [77] studied the influence of inlet CO_2 on phototrophic yield of biomass, lipid and chitin of *Cyclotella* sp. Consequently, lipid yield was found to increase proportionally with partial CO_2 pressure inlet until 3000 ppm [77]. Conversely, the chitin product was detected in a constrained silicon state and was not determined by partial CO_2 pressure [77]. Pegallapati et al. [72] obtained sufficient biomass yield in their experiment's first stage of operation whilst in the second stage extended lipid and fatty acid methyl ester production occurred. Tao et al. [78] applied fiber media in microalgae biofilm airlift PBs to improve biomass yield. The media capacity was 32.9 mg/g which led to a larger biomass yield (15.93 mg/L.d) being obtained, and lipid productivity (4.09 mg/L.d) better than that achieved in conventional PBs [78].

Regarding the effect of illumination pattern on biomass yield, Pavlik et al. [79] discovered that *C. vulgaris* 395 could achieve biomass productivity up to 0.40 g/L.d at an illumination intensity of 531 µmol/m.s. In addition, Mohsenpour and Willoughby [80] compared the impact of light's colour on microalgae growth. Red colour illumination enhanced biomass yield the most significantly in *C. vulgaris* and *Gloeothece membranacea*, their statistics being 1.49 - 1.92 and 2.27 g/L, respectively [80]. A green coloured light source favoured the chlorophyll content in *C. vulgaris* while *G. membranacea* and depended less on light source and culture density [80]. Janoska et al. [66] achieved *C. sorokiniana*'s growth rate of 0.1/h which was lower than other studies due to the unequal illumination in the foam bed. However, levels of P and sulfate ions

in PBs do emerge as a concern. The threat of bacterial contamination on microalgae growth was also reported [81].

With respect to the influence of nutrient conditions, Cabello et al. [82] concluded the photosynthetic activity was lower in N-starving condition than the N-redundant one. The highest biomass productivity of 0.78 g/L.d was predicted at the temperature of 35^{o}C and irradiance of 600 μmol/m^{2}s [82].

3.2.3 Pollutants removal

The column PBs are regularly implemented in nutrients removal and various results were reported consequently. Arias et al. [83] discovered that different nutrient ratio levels promoted sophisticated micro-organism and microalgae communities in closed PBs. The total inorganic N/inorganic P (21 mg N/L and 2 mg P/L), sufficient C supply and P volumetric load caused the proliferation of cyanobacteria over a period lasting 234 days [83]. Lee et al. [84] insisted carbon uptake was favoured under longer dark conditions while N and P consumption preferred light conditions. More specifically, chemical oxygen demand (COD), total nitrogen (TN) and total phosphorus (TP) were removed at 59-80%, 35-88% and 43-89%, respectively [84]. However, microalgae growth was restrained by nitrifying bacteria. Consequently, PBs in which the nitrifying process was inhibited, achieved higher growth rate and chlorophyll content [85]. Zhang et al. [86] improved nutrients removal efficiency via microalgae and bacteria consortium. The maximum COD, TN and TP removal efficiencies were 96.7%, 70.5% and 96.4%, respectively [86]. The granulation activity of bacteria was enhanced by green microalgae and resisted with temperature fluctuation.

The carbon source for microalgae cultivation is not only wastewater, but was also derived from CO_2 in ambient or polluted air of industrial activities [87]. Chen et al. [88] employed power plant fuel gas to cultivate microalgae; subsequently it emerged that *Spirulina platensis* could

uptake 2,234 kg CO_2 per year, which is equivalent to74 tons/ha.year. Furthermore, *C. vulgaris* also consumed 80% CO_2 in airlift PBs [89]. In the similar concept, Jacob-Lopes et al. [90] developed operational manuals to remove CO_2 in bubble column and airlift PBs. The air circulation method was suitable for small-scale treatment while two-stage-sequential PBs complied with industrial scale [90]. The removal efficiency and loading were beyond 52.5% and 12.217 g carbon/m^3 reactor.d, respectively, dealing with inlet CO_2 of 15% [90].

Regarding heavy metal, Arun et al. [48] observed complete removal of Cu (II); however, nitrate uptake rate declined, resulting in the decrease of biomass yield. The maximum biomass yield was 5.628 ± 0.05 g/L without Cu (II) in the culture while it dropped to 2.51 ± 0.01 g/L with Cu (II) concentration of 30 mg/L [48]. The heavy metals biosorption of microalgae happened at its speed from 15 to 30 minutes and reached equilibrium within 30 to 60 minutes [91]. The living carbohydrate-enriched biomass of *Arthrospira platensis* removed Cu^{2+} and Ni^{2+} more efficient (30%) than dry carbohydrate-enriched biomass [91]. The higher intracellular biosorption of living microalgae compared to the dry biomass was the responsible reason [91]. In another study, the dry biomass of *C. vulgaris* performed more distinctive than *A. platensis* [92]. The equilibrium biosorption records of *C. vulgaris*, removing Ni^{2+}, Pb^{2+} and Zn^{2+}, were 0.499, 0.634 and 0.664 mmol/g, respectively; whereas they were 0.354, 0.495 and 0.508 mmol/g , respectively, in the case of *A. platensis* [92].

With reference to PPCPs, *C. sorokiniana* was demonstrated to be effective in salicylic acid and paracetamol removal [93]. Through semicontinuous culture, 70% of those PPCPs has been removed from its initial concentration of 25 mg/L [93]. In detail, salicylic acid were eliminated 2.3 times faster than that of paracetamol, being 4 and 1 d^{-1}, respectively [93]. However, it has been reported that those PPCPs could transformed into metabolites known with more detrimental effect to human health and ecosystem. Thus, Ismail et al. [94] explored that *p*-

paracetamol, a metabolite of paracetamol, were efficiently removed 94% coupling 4 d hydraulic retention time (HRT) in a continuous illumination mode. Herein, the author insisted that 3 d HRT and dark environment performed a poor removal of *p*-paracetamol in which COD removal and toxicity test's results were unsatisfactory [94]. In another study, diclofenac were removed 99, 71 and 67% by *Scenedesmus obliquus*, *C. vulgaris* and *C. sorokiniana*, respectively in a batch microalgae-based PB within 10 d [95]. Interestingly, those PPCPs resulted in higher biomass growth rates of *C. sorokiniana* than the control experiment, indicating the nutrients-benefit offered [93]. This could be explained thanks to the mixotrophic characteristic of microalgae that both inorganic and organic carbon were well consumed for cells built up [93]. Nevertheless, this was not elucidated in other studies [94, 95]. In turn, Ismail et al. [94] and Escapa et al. [95] focused on the toxicity reduction and metabolites removal via microalgae-based PBs.

3.3 Tubular photobioreactors

The configurations of tubular PBs are plentiful in terms of bent, horizontal, vertical and spiral shapes. They are arranged as arrays/layers lying on or next to each other. These arrays/layers are connected and mixing is done through pumps or airlift systems. Therefore, tubular PBs have sufficient contact time for mass transfer.

3.3.1 Innovations of configurations and operations

Like other PB types, an attempt to re-configure tubular PBs was also carried out. As such, Gómez-Pérez et al. [96] applied a wall turbulence promoter in tubular PBs to reduce mixing energy consumption. The flow velocity from 0.1 to 0.3 m/s coupling inverse triangle shape, and wall turbulence promoter saved 60-80% energy utilization as compared to conventional PBs [96].

Tubular PBs involve a number of operational parameters (e.g. tube arrangement, DO, nutrient distribution, energy and illumination). Thus the optimization of these conditions is critical, despite it being more complicated than other PB types.

Henrard et al. [97] operated a semicontinuous mode in vertical tubular PBs. These authors insisted the proper combination of blend concentration (1.0 g/L), renewal rate of medium (30-50%) and bicarbonate concentration (1.0 g/L) resulted in expected biomass yield [97]. This result was ideal for industrial scale, fixing the drawback of high cost related to batch mode operation. Slegers et al. [98] examined the contribution of reactor dimension, sunlight condition and microalgae characteristics in horizontal and vertical tubular PBs. As a consequence, vertical PBs enjoyed much higher productivity than horizontal ones, e.g. 70% compared to 25% [98]. Furthermore, geographical locations decided the efficiency of PBs. In the Netherlands, distances between tubes were 0.05 and 0.25 m for horizontal and vertical systems, respectively, while they were 0.2 and 0.15m in Algeria [98]. Slegers et al. [98] suggested that having reflection material, bringing more illumination, on the ground could improve system performance. Iluz and Abu-Ghosh [99] constructed a fluctuating illumination concept for use in combined-light PBs. The biomass productivity increased by 55% while light-to-biomass conversion efficiency improved and the fluctuating frequency was 60 Hz [99].

The disadvantage of tubular PBs is the considerable amount of power consumption due to mixing of media in connected long continuous tubes, ranging from 100 to 500 W/m^3 [1]. Alternatively, the twisted tubular PBs with swirl flow were proposed to reduce energy consumption between 38% and 77% [100].

3.3.2 Microalgae growth and control

Regarding microalgae biomass yield in tubular PBs, there have been different outcomes in relation with this matter. Concas et al. [101] studied the influence of dissolved N on autotrophic

growth and lipid accumulation of *C. sorokiniana*. The maximum growth rate of 0.52 g/L and lipid accumulation of 25 %wt were achieved through experimental data while the modelling obtained similar outcomes [101]. da Silva et al. [102] confirmed the distinct performance of horizontal PBs compared to open pond, shaken flask and helicoidal PBs. Specifically, maximum biomass concentration of *A. platensis* was 8.44 ± 0.13 g/L at a surface/volume ratio of 1.94/cm [102]. In another effort, Binnal and Babu [103] stated optimal operating conditions of pH, temperature, light intensity, photoperiod, CO_2 concentration and aeration rate were 6.51, 28.63ºC, 5.31 klux, 15.36:8.64h, 6.26% (v/v) and 2.92 lpm, respectively, for *Chlorella protothecoides*. In this scenario, the level of N starvation achieved lipid productivity of 274.15 mg/L.d which was 3.94 times higher than N surplus state [103]. This agreed with the findings of other studies [104, 105]. Nonetheless, the carbon fixation rates were quite similar in both conditions.

Saeid and Chojnacka [106] compared the performance of laboratory scale (0.5 m^3) and outdoor semi-technical scale (10 m^3) units. The biomass yield of *Spirulina maxima* was achieved at 0.299 and 0.43/d in laboratory scale and semi-technical scale PBs, respectively [106]. The difference in biomass yield stemmed from higher light intensity and temperature in outdoor greenhouse scenarios.

3.3.3 Pollutants removal

Compared to other PBs type, tubular PBs implemented in pollutants removal were rarely progressed in literature and the number of reported pollutants were also limited.

In a lab scale tubular PBs, Binnal and Babu [103] reported CO_2 fixation rate was maximized to 273.66 mg/L.d under N starvation condition. Via response surface methodology, the optimal operating conditions were determined including: pH of 6.51, temperature of 28.63ºC, light

intensity of 5.31 klux, photoperiod of 15.36:8.64 h, CO_2 concentration in air of 6.26% (v/v) and aeration rate of 2.92 lpm [103].

For PPCPs treatment, Kang et al. [107] in their study employed periphyton PBs to eliminate PPCPs. Bisphenol A was removed in significant amounts, ranging from 72% to 86.4% while hydrochlorothiazide, ibuprofen, carbamazepine and gemfibrozil were moderately treated, varying from 6.45% to 48.7% [107]. The authors concluded that microbial community contributed more to PPCPs removal than microalgae biomass [107]. The periodic and low irradiance illumination influenced the extent of PPCPs removal [107].

3.4 Soft-frame photobioreactors

Most PBs are made of hard materials and are fixed permanently throughout their operational life. The soft-frame PBs are space-saving, flexible, foldable, and mobile. They are designed in an array of configurations in either hanging on rack, floating on water or lying on the ground (Fig. 5). The manufacturing material options also vary from ethylene vinyl acetate/low density polyethylene (EVA/LDPE), and polyethylene to polytetrafluoroethylene (PTFE). Compared to other PBs, the applications of soft-frame PBs are modest but increasingly becoming more attractive recently.

[Insert Figure 5]

3.4.1 Innovations of configurations and operations

In a lab scale soft-frame PB, Hamano et al. [108] attached microalgae on cellulosic sheets or on PTFE membrane sheets, then cultivated it in PBs. The nutrient was supplied via a capillary mechanism through the cellulosic sheet; thus, no energy for mixing was required [108]. Unfortunately, constraints with the high PTFE material costs obstructed the commercialization of this technology. In large-scale operations, Chemodanov et al. [8] integrated PE PBs into building, using sunlight as a illumination source. However, the growth rates widely fluctuated

for not clear reason. In a similar concept, Hom-Diaz et al. [109] and García-Galán et al. [110] constructed full scale soft-frame PBs made of PE for toilet wastewater and agricultural run-off treatment, respectively. Notably, those PBs were originally called horizontal multi-tubular PBs; however, they also could be categorized as soft-frame PBs thanks to their foldable and soft material. Soft-frame PBs are promising and have much potential for industrial-scale production. Nevertheless, there are some drawbacks, including insufficient illumination efficiency, and the cost and longevity of materials. The inadequate mixing is another challenge due to formation of a dead zone inside.

Referring to energy matter, Jones et al. [111] optimized energy consumption in EVA/LDPE PBs. The surface aeration and rocking platform mixing methods were initiated to replace sparging. The power input was minimized at 57.6 to 903.3 W/m^3 which did not disturb microalgae growth [111].

3.4.2 Microalgae growth and control

In the wave PBs, Jones et al. [111] cultivated maximum biomass concentration of 2.25 g/L in EVA/LDPE PBs. The wave PBs achieved a higher biomass yield than air sparging PBs. Hamano et al. [108] recorded a biomass yield of 8-10 g/m^2.d. Interestingly, Chemodanov et al. [8] calculated maximum accumulated energy rates of *Cladophora* sp., *Ulva compressa* and *Ulva rigida* in polyethylene PBs were 0.033, 0.081 and 0.029 Wh/L.d, respectively [8]. Schreiber et al. [112] cultivated microalgae in three types of commercial PBs assigned them in hanging situation. The biomass yield ranged from 0.3 to 1.5 kg/m^3 and this dominated 2/3 of maximum growth rate at an irradiation intensity of 50 mol photons/m^2.d [112]. These authors noticed that robust modular-based PBs could augment both biomass yield and lipid accumulation under N starvation conditions. As for microalgae growth this was obstructed due to the shadow effect of surrounding buildings.

3.4.3 Pollutants removal

Similar to tubular PBs, previous published literature in pollutants removal in soft-frame PBs is modest. It is likely soft-frame PBs were recently favourable in culturing microalgae biomass yield option, rather than pollutants treatment. In the full scale soft-frame PB, Hom-Diaz et al. [109] reported that $N\text{-}NH_4^+$, TP and COD from toilet wastewater were removed beyond 80%. For PPCPs removal, substantial removal efficiencies of anti-inflammatory drugs (ibuprofen, acetaminophen, salicylic acid, and codeine) (98%), diuretics hydrochlorothiazide (84%) and furosemide (100%) were observed [109]. However, the antibiotics, such as azithromycin, ciprofloxacin, ofloxacin and erythromycin) could be removed only 48% in this PBs [109]. The major requirements of HRT were 8 days during period I and 12 days during period II [109]. In a latter study, Parladé et al. [113] reused the PBs system of Hom-Diaz et al. [109] to evaluate 17β-estradiol removal efficiency by microalgae-bacterial consortium. The author revealed that 17β-estradiol was completely removed in 12h; nevertheless, estrone is detected as metabolite [113].

García-Galán et al. [110] managed the full scale horizontal tubular PBs (7.2 m^3) with agricultural run-off. This system was shown to be successful in removing N and P of 84-95 and 100%, respectively [110]. The contribution of environmental factors, especially solar illumination, in outdoor condition was insisted since the biomass growth was recorded without significant change of nutrients levels [110]. Thus, solar illumination was a reasonable explain for the result. The full scale PBs of García-Galán et al. [110] removed the synthetic musk fragrances, such as tonalide and galaxolide, 73 and 68%, respectively, while anti-inflammatory compound (e.g., diclofenac) was eliminated 61% after 4 months operation.

3.5 Hybrid photobioreactors

3.5.1 Innovations of configurations and operations

Hybrid PBs are defined in this review as the combination and/or integration of the above-mentioned four PBs or with other technologies (e.g., membrane process) resulting in PBs' volume reduction, higher biomass yield and pollutants removal efficacy. The hybrid PBs were developed by exploiting the prominent characteristics of traditional PBs [114]. Soman and Shastri [9] combined the advantage of flat plate and tubular PBs, resulting in a novel design. The tubular zone was operated in the cylindrical core of a rectangular tube while two surrounding baffles were connected to the tube and served as a flat plate mechanism where the flow came down [9]. This type has 7% larger surface to volume ratio and premium flow regime [9]. The light/dark frequency was 0.14 Hz which was better than the conventional one [9]. This may reduce operational and material costs for further upscaling activity. Provided that attached cultivation process received more advantages than suspended one in biomass harvest, Xu et al. [115] proposed a capillary-driven PB which the nutrients and water were fed via capillarity into a polyester microfibers media. This PB consequently achieved biomass with higher carbohydrates content but much lower protein; so it was stated to be applicable to biofuel production [115].

Other innovative types of PBs were developed to reduce reactor size and maximize biomass yield. These designs and technologies adapt to various geographical locations. Dogaris et al. [14] developed floating horizontal PBs from plastic film in modular configuration. It included two plastic films in the top and bottom surfaces of PBs which sealed each other and had two air lift vertical units attached to them [14]. In other work, Pruvost et al. [116] aimed to achieve high volumetric performance in thin-film (AlgoFilm©) PBs as done in the fermentation process. The thin culture layer (1.5-2mm) provided an illumination area up to 500 m^2/m^3 created by an intensification mechanism [116]. Similarly, a light guide plate, modified with

SiO_2 chitosan medium, was integrated into the PBs to enhance biohydrogen gas production [117].

Other authors combined the membrane process and PBs, terming them membrane PBs [118-120]. For instance, Chang et al. [68] initiated ion-exchange membrane PBs which divided wastewater sources and microalgae into separate chambers. The nutrients (e.g. N, P) permeated through an ion exchange membrane into the microalgae chamber. This design alleviated the negative impact of contaminants in wastewater on microalgae growth; however, the high cost of ion exchange membrane was the main constraint in upscaling [68]. The technical problem associated with membrane PBs was fouling [121-124]. Recently, membrane fouling has been studied in-depth by researchers. For instance, the ceramic membrane operating at HRT of 6.5h possessed more significant fouling rate compared to the HRT of 24 and 72h [123]. The fouling of hollow fiber membrane was alleviated while combining microalgae and sludge bioreactor [124]. The released O_2 from algae photosynthesis reduced bacteria death, which in turn brought benefit to membrane fouling.

With respect to large-scale application, a membrane PB consisted of flat plate PBs and hollow fibre ultrafiltration membrane was done by Viruela et al. [125]. Also, a sequencing membrane PBs treating secondary effluent wastewater was established by Sheng et al. [10].

3.5.2 Microalgae growth and control

In the afore-mentioned capillary-driven PB, the highest biomass yield per footprint area was over 121.5 g/m^2, and the highest biomass productivity was about 10 $g/m^2.d$ [115]. It can be seen that the biomass productivity in this study was 14 times higher than that of Ozkan et al. [55], given 0.71 $g/m^2.d$.

Referring to membrane PBs, Bilad et al. [126] maintained the proper microalgae concentration in PBs by employing a membrane which could retain more than 50% biomass. This technology could generate more biomass nine times larger than conventional units while also reducing 77% of water footprint [126]. In a floating horizontal PBs, Dogaris et al. [14] documented biomass concentrations of 4.0 and 4.3 g/L in indoor and outdoor conditions, respectively. Gao et al. [36] found biomass yield proportionally rose within certain mixing rate ranges. The equal distribution of microalgae and gas bubble were the key factors. Pruvost et al. [116] obtained biomass productivity of 7.07 kg/m^3.d in thin-film solar PBs which was higher than in other literature reports. Moreover, there was an increase in the production of biomass.

The lipid content of *Phaeodactylum tricornutum* in India reached 31% DW with biodiesel productivity of 34,386 g/y [11]. Yet, the high irradiance of solar light might bring about light inhibition which could damage microalgae cells. With reference to commercial PBs, Fuentes-Grünewald et al. [127] evaluated *Amphidinium carterae* as a prominent candidate in closed systems (indoor and outdoor conditions) and under semi-continuous mode. Furthermore, pigment products (e.g. ω3, ω6 fatty acids, peridinin, β-carotene) indicated a revenue-rising potential.

3.5.3 Pollutants removal

The utilization and combination of membrane and PBs technologies can considerably enhance nutrients removal efficiency. These include an array of membrane types: biofilm, suspended process, microfiltration, forward osmosis and ultrafiltration. In biofilm membrane PBs, TN (82.5%) and TP (85.9%) in secondary effluent were removed; and these amounts were higher than suspended growth membrane PBs [118]. The membrane PBs could retain microalgae, leading to low suspended solid concentration (0.28 mg/L) in the effluent [118]. In another study, Gao et al. [119] contended that hollow fiber microfiltration membrane PBs could remove TN and TP at 86.1% and 82.7%, respectively, in aquaculture wastewater. The ammonia

concentration in effluent was considerably low at 0.002 mg/L [119]. Later on, the operation of this membrane PBs was optimized through the adjustment of HRT and biomass retention time, being 2 days and 21.1 days, respectively [128]. The removal efficiencies of TN and TP were improved to 81.4% and 90.8%, respectively [128]. The inlet N and P concentration in this study were two-fold higher than the wastewater source of Gao et al. [119].

Regarding forward osmosis PBs, it could treat N and P at 86-99 and 100%, respectively, which are higher amounts than microfiltration PBs of 48-97 and 46%, respectively [120]. Evidence suggests that forward osmosis PBs consumed more than 3.5 to 4.5 times more energy than microfiltration PBs [120]. Fu et al. [129] focused on adjusting nutrient supply rate in anion exchange membrane PBs. The optimal inlet N and P supply rate was 19.0 mg N/L.d and 4.2 mg P/L.d, respectively, resulting in biomass concentration from 2.98 to 4.38 mg/L [129]. This achievement was 129.2% higher than what could be done in conventional PBs [129]. Also, organic/inorganic carbon and ammonium/nitrate (NH_4^+-N/NO_3^--N) ratios could determine nutrient removal efficiency [130], Podevin et al. [131] operated full-scale air-lift PBs coupling wastewater ultrafiltration system and harvesting microfiltration system. Nutrients (e.g. H_2PO_4-P and NH_4^+-N) were not detected after 4 days while COD decreased from 230 to 30.25 mg/L [131].

Apart from membrane processes, Lee and Han [132] constructed integrated systems, including anaerobic digestion, expended granular sludge bed and combined microbial-microalgae PBs, to treat swine wastewater. The volatile solid and COD were removed at amounts of 99.3% and 99.7%, respectively [132]. The TN, NH_4^+-N and TP were efficiently treated at amounts of 98.8%, 98.4%, and 93.5%, respectively [132]. Furthermore, Lee and Han [132] qualified and quantified the contribution of PBs in VS, COD, TN, NH_4^+-N and TP removal efficiency. The recorded percentages were 0.4%, 6.0%, 27.3%, 32.6% and 11.8%, respectively [132]. Maza-

Márquez et al. [133] treated olive washing water with tubular PBs, coupling the activated carbon pre-treatment column. The contaminants, included phenols, COD, biochemical oxygen demand (5 d), turbidity and colour. The amounts removed were 94.84 ± 0.55%, 85.86 ± 1.24%, 99.12 ± 0.17%, 95.86 ± 0.98 % and 87.24 ± 0.91%, respectively [133]. According to Binnal and Babu [134], COD, TN and TP removal efficiencies were 78.03%, 100% and 100%, respectively, in a hybrid system of column and tubular PBs. These removal efficiencies were achieved at light intensity 6 klux, dark/light photoperiod 8h:16h, CO_2 concentration 6%, temperature 25ºC and aeration rate 3 lpm [134].

4. Comparisons of photobioreactors and discussions

It is clear that most authors initially optimized the operation of PBs to favour illumination pattern, fluid dynamic and mass transfer processes. This resulted in maximizing biomass yield, augmenting pollutants removal efficiency, reducing costs and saving energy. Furthermore, it is evident that configurations were modified and combined with other technologies. Some research work encompassed modelling and experiments for mutual validation. However, each type of PB has its advantages and drawbacks which are summarized in Table 3.

[Insert Table 3]

In the effort to compare these PBs, Yadala and Cremaschi [11] studied the designs of tubular, column and flat plate PBs. Through the modelling approach, horizontal tubular PB was the best design with minimum costs. The proposed diameter and length of this reactor were 0.05 and 15.12 m, respectively [11]. However, these horizontal tubular PBs must couple with *P. tricornutum* species and locate in Hyderabad (India), where the climate is favorable for microalgae cultivation. Furthermore, López et al. [12] experimented a comparison study of tubular and bubble column PBs in outdoor conditions. Consequently, the tubular PBs received illumination 2.5 times higher than bubble column PBs thanks to its higher illuminated surface

and horizontal configuration [12]. Concerning biomass yield and productivity, the tubular PBs perceived 7 g/L and 0.55 g/L.d, respectively; whereas bubble column PBs were observed 0.41 g/L and 0.12 g/L.d, respectively [12]. In this study, the energy balance analysis was necessary for further comparison; nevertheless, it was not reported. In contrast, Mirón et al. [13] confirmed the more advance of bubble column PBs compared to horizontal tubular PBs via experiments and engineering analysis. The reason was that bubble column suffered less photoinhibition, and able to maintain sufficient illumination during low light intensity period [13]. In addition, bubble column PBs was easy to scale up and offered homogenous microalgae cultures. The horizontal tubular PBs were concluded to be impractical in large-scale and commercial applications [13]. However, it was observed that horizontal tubular PBs have been evidently applied in full scale in section 3.3.

With respect to hybrid PBs, there was no extensive comparison done between hybrid PBs and other PBs types. Any comparisons made from fragmental studies would gain relative results and may pose potential errors due to the discrepancies in operating conditions, applied microalgae strain. Nevertheless, the membrane PBs as a particular sub-class of hybrid PBs were elsewhere compared to membrane bioreactor [130, 135]. Succinctly, the integration of membrane in PBs offered more opportunity to operate at higher dilution rate and minimize wash-out problem given higher biomass productivity [135]. In the case of bubble column PBs, illumination was provided to microalgae cells more sufficiently if PB's size was reduced in some extent. Alternatively, it could be done via the combination with membrane process. The operation and maintenance (O&M) cost of membrane PBs was estimated at 0.113 \$/m^3 that of significantly lower than conventional technology (0.65-0.96 \$/m^3) [10]. It indicated a chance for upscaling in space-limited places.

Overall, this review found flat plate PBs have the highest biomass concentration (7.5 - 96.4 g/L), followed by the column PBs with internal illumination pattern (19.78 g/L). The other types of PB achieved biomass concentration at around 4 g/L (Table 4). It can be seen that the reported biomass yield of flat plate PBs were 5 to 20 times higher than other types. Nevertheless, it is difficult to conclude which type is the best due to the lack of uniform data from biomass productivity. The biomass concentration in the study of Ozkan et al. [55] was exceptionally high but the productivity was only 0.71 g/m^2. Therefore, the impact of other factors, such as specific microalgae strains, geographical conditions, operation efficiency, energy consumption, and cost analysis must also be considered [18, 136, 137].

[Insert Table 4]

With reference to pollutants treatment, different microalgae strains require different levels of nutrients and possess various contaminants removal efficiencies. Microalgae can also improve the removal of contaminants from heavy metals, PPCPs. Thus, a prior screening of microalgae species is important before cultivating them in PBs [138, 139]. Amongst microalgae species, the *C. vulgaris* and *Chlorella* sp. were preferred to be applied in PBs which able to deal types of pollutants (Table 5). The wastewater for microalgae cultivation stems from many sources, for instance: domestic wastewater, livestock wastewater, industrial wastewater or secondary, and/or tertiary effluent from wastewater treatment plants. Therefore, levels of inlet pollutants concentration fluctuate accordingly. The maximum inlet respective COD, TN and TP concentrations are recorded as 3700, 162 and 209 mg/l [140]. There is limited explanation regarding the benefits of PBs' configurations to pollutant removal efficiency [62, 85]. However, biomass yield, which directly receive those benefits from PBs, and levels of pollutants removal possess a correlation. The PB's configurations condition illumination, temperature, hydrodynamic pattern; thus, microalgae consume pollutants extensively. The

pollutants removal efficiency is enhanced consequently. Judging the efficiency of PBs based on removal efficiency is not that accurate, the initial pollutants loading, operating conditions, microalgae trains and climate conditions are recommended to accompany.

[Insert Table 5]

In this regards, wastewater treatment was employed preferably in open systems, such as high rate algae ponds; whereas the closed systems (e.g. PBs) were more common in achieving the valuable products (e.g. biofuels, pharmaceuticals) [5]. However, our review indicated that the applications of PBs in wastewater treatment sector have been applied widespread and grown up constantly. The removal efficiencies of TN, TP and COD in microalgae-based PBs reportedly reached to 100%. The treatment of heavy metals and micro-pollutants by PBs is promising although the number of studied heavy metals and PPCPs were still modest.

5. Future perspectives on the development of photobioreactors

Many innovative configurations have been researched such as multi-column, modular flat plate, and hybrid systems [9, 51, 65, 68]. The high energy cost and adjustments made to the local conditions (temperature, light and climate) are the main constraints. Alternatively, Pruvost et al. [141] integrated vertical flat panel PBs into building's facades in Nantes (France). This approach helped to increase the illumination from solar and employed CO_2 emission from building to cultivate microalgae. By applying thermal regulation process, total energy consumption was saved 70% [141]. Unfortunately, the energy balance was still negative. Chemodanov et al. [8] also integrated soft-frame PBs into buildings. This strategy has been assisted by softwares [142]. Two types of flat panel and tubular PBs were assessed by Geographic Information Systems for their energy production capacity. Subsequently, they were integrated into a built environment and analysed for the energy balance via the Building Information Model. However, no data was applied to validate the model. PBs can receive more

solar illumination via the assist of Green Solar Collector [143] or Dye-sensitized Solar Cells [144], fixing the drawback of insufficient light in low latitude locations. These devices could be operated at the higher fluctuation of sun's angles and improved sunlight capturing efficiency 89% [143, 144]. Some researchers like Eltayeb et al. [69] and Lee and Han [132] have developed PBs so that they are sustainable concepts and result in zero waste discharge.

The collocation of microalgae-based PBs and building emerges as new trend in green building in the recent years. Amongst these configurations, flat plate PBs are the most common in architecture and infrastructure designs (Fig. 6).

[Insert Figure 6]

To construct a PB-based building, the flat plate microalgae-based PBs were entirely collocated in the building's facade positions. By doing so, it would benefit microalgae growth with adequate sunlight and temperature; and also creating shade for the interior of the building. In addition, the PBs could retain the heat energy and returned it for building. Thus, these approaches should be further investigated and refined, in order to obtain revenues from biomass and by-products whilst contaminants are treated and reduced. The collocation of PBs and constructions is the encouraging outlook of PBs which offers the following advantages:

- Wastes from other processes can be applied as inputs in PBs
- Centralized the operation and control processes
- Cost cut-off by producing multiple products
- Retaining heat for internal building heating

As reported that the building encompassed multi-functions of bioenergy production, heating, algae cultivation, it is a technical-sophisticated and perhaps a costly building. Another concern is raised whether or not to construct this building in high latitude regions due to the effect of low temperature to algae growth. Coming across those issues, this is an encouraging and

pioneer green building with microalgae-based PBs. The criteria which are recommended for the integration of PBs and buildings illustrated in Table 6.

[Insert Table 6]

The most serious issues are concerned with upscaling. While the performance of PBs is promising in laboratory and pilot-scale contexts, industrial-scale PBs still requires much research and development. Current research is being undertaken by institutes and small private companies, so the large-scale systems are rare or limited in their functions. For instance, flat plate PBs are integrated with plastic disposable bags PBs [1]. This particular system needs the frequent replacement of bags due to leakage, fouling, and over-heating being serious problems [1]. The high cost of microalgae harvesting, biofuel production and energy consumption for mixing was another indirect reason for upscale activity [145, 146]. Furthermore, the large-scale PBs require sufficient reactors' volume and thickness of materials. Unfortunately, the oversize reactor and thickness discourage light transmittance and mixing efficiency. As the design of PBs further develops, coupled with the strong support of modelling tools the operating conditions will function more efficiently. At present, there is limited specifically accepted guideline for designing and constructing PBs. This process still in the trial and error stages. For instance, the design manuals for upscaling of the flat plate and tubular PBs were developed elsewhere [57, 98]. Fuente et al. [34] also developed illumination modelling that can be upscaled. The modelling approaches were advised to apply, rather than experimental works, in the case there were more than six considered variables. While mixing reactors for yeast and bacteria growth have standard geometries, the control of microalgae culture continues to be complicated [147]. The upscaling of PBs is promising as the environmental and energy friendly strategies and being observed with a significant growth up in the upcoming years [148, 149].

Referring to economic concern, the total cost of PBs decided by construction, maintenance and operating expenditures. The average cost of vertical PBs was €30 at the scale of 500 m^2 [5], illustrating in Table 7.

[Insert Table 7]

The payback period of constructing PBs can be achieved from 9 to 13 years [150]. In the case of bio-fertilizer application, it is shortened to 7 years thanks to more economic value [150]. Cheaper costs can be achieved via several options. The use of sunlight could reduce US$307 per 0.5 kg dry cell [150]. Total production cost falls when employing larger reactors (US$121 per 0.5 kg dry cell in 200 L reactor compared to uS$197 per 0.5 kg dry cell in 17 L unit) [150]. The reuse of a spent medium only saved US$8 per 0.5 kg dry cell [150]. Nonetheless these methods did cause a fall in the growth of microalgae. Therefore, it is evident that stand-alone PBs are not currently meeting the objectives of economic and renewable energy targets.

6. Conclusion

Generally, PBs are a promising selection in which many benefits are gained. The control of microalgae growth in PBs is far better compared to open or natural eco-systems. According to the review objectives, the following conclusions are made:

(1) The models discussed here mostly focus on estimating biomass yield, studying the effect of illumination patterns and calculating pollutant assimilation rates in PBs. Research regard microalgae growth is dynamic in that there are different outcomes between experiments and modelling works, being of 10%. The advised biomass concentration in PBs was 0.2 to 2 g/L. Monod model was a classical one remaining some shortcomings in the temperature, light intensity and internal substrate utilization that fixed by Droop, Luedeking–Piret and modified Droop models.

(2) Most research optimized the operation of PBs to favour fluid dynamics, illumination patterns and mass transfer. This resulted in maximizing the biomass yield, reducing costs and saving energy. Furthermore, the configurations were modified and combined with other technologies, such as membrane. For example, a membrane bubble column PBs could reduce reactor size and diminish O&M cost. The new-born soft-frame PBs were known to be foldable, movable and flexible compared to other types.

(3) Flat plate PBs experienced the highest biomass yield up to 96.4 g/L being 5 to 20 times higher than other PBs types. However, this process did depend on other factors, e.g. microalgae strains, local and operating conditions. The performance of PBs was promising at laboratory scale and pilot scale, but full- scale operations and construction remained important challenges. Attached cultivation process was observed to have higher biomass yield than the suspended one.

(4) A wide range of contaminants could be treated by PBs (e.g. nutrients, heavy metals and PPCPs). The removal efficiencies were significant, for example up to 99% and 100% for TN and TP, respectively, and 100% for COD and 95% for PPCPs. The proper C:N:P in the influent was important. In such a case, metabolites of PPCPs could be managed by soft-frame PBs in a proper HRT (3 d) and continuous illumination.

(5) Upscaling PBs was still a challenging task. Flat plate PBs were the most favorable in architecture and infrastructure designs. The average cost of 500 m^2 PBs was 30$ while the payback period was from 9 to 13 years. Currently, the stand-alone PBs did not meet the objectives of renewable energy and economic targets.

Acknowledgements

This review research was supported by the Centre for Technology in Water and Wastewater, University of Technology, Sydney (UTS, RIA NGO) and in part by grants from the Korea

Ministry of Environment as an “Algae Monitoring & Removing Utilization Technology” (Project No. 2015001790001) and Joint Research Centre for Protective Infrastructure Technology and Environmental Green Bioprocess (UTS and Tianjin Chengjian University).

References

[1] Posten, C. and Walter, C., Microalgal Biotechnology: Potential and Production. 2012.

[2] Sierra, E., Acién, F.G., Fernández, J.M., García, J.L., González, C., and Molina, E. (2008) Characterization of a flat plate photobioreactor for the production of microalgae. Chem. Eng. J. 138 (1) 136-147.

[3] Wang, B., Lan, C.Q., and Horsman, M. (2012) Closed photobioreactors for production of microalgal biomasses. Biotechnol. Adv. 30 (4) 904-912.

[4] Suh, I.S. and Lee, C.-G. (2003) Photobioreactor engineering: Design and performance. Biotechnol. Bioproc. E. 8 (6) 313.

[5] Torgal, F.P., Buratti, C., Kalaiselvam, S., Granqvist, C.-G., and Ivanov, V. (2016) Nano and Biotech Based Materials for Energy Building Efficiency. Springer International Publishing.

[6] Huang, Q., Jiang, F., Wang, L., and Yang, C. (2017) Design of Photobioreactors for Mass Cultivation of Photosynthetic Organisms. Engineering. 3 (3) 318-329.

[7] Pires, J.C.M., Alvim-Ferraz, M.C.M., and Martins, F.G. (2017) Photobioreactor design for microalgae production through computational fluid dynamics: A review. Renew. Sust. Energ. Rev. 79 (Supplement C) 248-254.

[8] Chemodanov, A., Robin, A., and Golberg, A. (2017) Design of marine macroalgae photobioreactor integrated into building to support seagriculture for biorefinery and bioeconomy. Bioresour. Technol. 241 1084-1093.

[9] Soman, A. and Shastri, Y. (2015) Optimization of novel photobioreactor design using computational fluid dynamics. Appl. Energ. 140 246-255.

[10] Sheng, A.L.K., Bilad, M.R., Osman, N.B., and Arahman, N. (2017) Sequencing batch membrane photobioreactor for real secondary effluent polishing using native microalgae: Process performance and full-scale projection. J. Cleaner Prod. 168 708-715.

[11] Yadala, S. and Cremaschi, S. (2014) Design and optimization of artificial cultivation units for algae production. Energy. 78 23-39.

[12] López, M.C.G.-M., Sánchez, E.D.R., López, J.L.C., Fernández, F.G.A., Sevilla, J.M.F., Rivas, J., Guerrero, M.G., and Grima, E.M. (2006) Comparative analysis of the outdoor culture of *Haematococcus pluvialis* in tubular and bubble column photobioreactors. J. Biotechnol. 123 (3) 329-342.

[13] Mirón, A.S., Gómez, A.C., Camacho, F.G., Grima, E.M., and Chisti, Y., Comparative evaluation of compact photobioreactors for large-scale monoculture of microalgae, in Prog. Ind. Microbiol., Osinga, R., Tramper, J., Burgess, J.G., and Wijffels, R.H., Editors. 1999, Elsevier. p. 249-270.

[14] Dogaris, I., Welch, M., Meiser, A., Walmsley, L., and Philippidis, G. (2015) A novel horizontal photobioreactor for high-density cultivation of microalgae. Bioresour. Technol. 198 316-324.

[15] Al Ketife, A.M.D., Judd, S., and Znad, H. (2016) A mathematical model for carbon fixation and nutrient removal by an algal photobioreactor. Chem. Eng. Sci. 153 354-362.

[16] Zhang, D., Wan, M., del Rio-Chanona, E.A., Huang, J., Wang, W., Li, Y., and Vassiliadis, V.S. (2016) Dynamic modelling of *Haematococcus pluvialis*

photoinduction for astaxanthin production in both attached and suspended photobioreactors. Algal Res. 13 69-78.

[17] Bitog, J.P., Lee, I.B., Lee, C.G., Kim, K.S., Hwang, H.S., Hong, S.W., Seo, I.H., Kwon, K.S., and Mostafa, E. (2011) Application of computational fluid dynamics for modeling and designing photobioreactors for microalgae production: A review. Comput. Electron. Agric. 76 (2) 131-147.

[18] Vasumathi, K.K., Premalatha, M., and Subramanian, P. (2012) Parameters influencing the design of photobioreactor for the growth of microalgae. Renew. Sust. Energ. Rev. 16 (7) 5443-5450.

[19] Luo, Y., Le-Clech, P., and Henderson, R.K. (2017) Simultaneous microalgae cultivation and wastewater treatment in submerged membrane photobioreactors: A review. Algal Res. 24 425-437.

[20] Elrayies, G.M. (2018) Microalgae: Prospects for greener future buildings. Renew. Sust. Energ. Rev. 81 1175-1191.

[21] Shriwastav, A., Thomas, J., and Bose, P. (2017) A comprehensive mechanistic model for simulating algal growth dynamics in photobioreactors. Bioresour. Technol. 233 7-14.

[22] Lee, E., Pruvost, J., He, X., Munipalli, R., and Pilon, L. (2014) Design tool and guidelines for outdoor photobioreactors. Chem. Eng. Sci. 106 18-29.

[23] Das, A., Basu, S., Ghosh, S., Dairkee, U.K., and Chowdhury, R. (2018) Mathematical modelling of flat plate biofilm photobioreactors with circular and rectangular configurations. Biosys. Eng. 174 66-79.

[24] Diehl, S., Zambrano, J., and Carlsson, B. (2018) Analysis of photobioreactors in series. Math. Biosci.

[25] Perez-Castro, A., Sanchez-Moreno, J., and Castilla, M. (2017) PhotoBioLib: A Modelica library for modeling and simulation of large-scale photobioreactors. Comput. Chem. Eng. 98 12-20.

[26] Ye, C., Shen, Z., Zhang, T., Fan, M., Lei, Y., and Zhang, J. (2011) Long-term joint effect of nutrients and temperature increase on algal growth in Lake Taihu, China. Journal of Environmental Sciences. 23 (2) 222-227.

[27] Concas, A., Steriti, A., Pisu, M., and Cao, G. (2014) Comprehensive modeling and investigation of the effect of iron on the growth rate and lipid accumulation of *Chlorella vulgaris* cultured in batch photobioreactors. Bioresour. Technol. 153 340-350.

[28] García-Camacho, F., Sánchez-Mirón, A., Molina-Grima, E., Camacho-Rubio, F., and Merchuck, J.C. (2012) A mechanistic model of photosynthesis in microalgae including photoacclimation dynamics. J. Theor. Biol. 304 (Supplement C) 1-15.

[29] Rubio, F.C., Camacho, F.G., Sevilla, J.M., Chisti, Y., and Grima, E.M. (2003) A mechanistic model of photosynthesis in microalgae. Biotechnol. Bioeng. 81 (4) 459-73.

[30] Brindley, C., Jiménez-Ruíz, N., Acién, F.G., and Fernández-Sevilla, J.M. (2016) Light regime optimization in photobioreactors using a dynamic photosynthesis model. Algal Res. 16 (Supplement C) 399-408.

[31] Murphy, T.E. and Berberoğlu, H. (2011) Effect of algae pigmentation on photobioreactor productivity and scale-up: A light transfer perspective. J. Quant. Spectrosc. Radiat. Transfer. 112 (18) 2826-2834.

[32] Kong, B. and Vigil, R.D. (2014) Simulation of photosynthetically active radiation distribution in algal photobioreactors using a multidimensional spectral radiation model. Bioresour. Technol. 158 141-148.

[33] Jiménez-González, A., Adam-Medina, M., Franco-Nava, M.A., and Guerrero-Ramírez, G.V. (2017) Grey-box model identification of temperature dynamics in a photobioreactor. Chem. Eng. Res. Des. 121 125-133.

[34] Fuente, D., Keller, J., Conejero, J.A., Rögner, M., Rexroth, S., and Urchueguía, J.F. (2017) Light distribution and spectral composition within cultures of micro-algae: Quantitative modelling of the light field in photobioreactors. Algal Res. 23 166-177.

[35] Marshall, J.S. and Sala, K. (2011) A stochastic Lagrangian approach for simulating the effect of turbulent mixing on algae growth rate in a photobioreactor. Chem. Eng. Sci. 66 (3) 384-392.

[36] Gao, X., Kong, B., and Dennis Vigil, R. (2017) Comprehensive computational model for combining fluid hydrodynamics, light transport and biomass growth in a Taylor vortex algal photobioreactor: Eulerian approach. Algal Res. 24, Part A 1-8.

[37] Fernández, I., Acién, F.G., Fernández, J.M., Guzmán, J.L., Magán, J.J., and Berenguel, M. (2012) Dynamic model of microalgal production in tubular photobioreactors. Bioresour. Technol. 126 172-181.

[38] Shriwastav, A., Ashok, V., Thomas, J., and Bose, P. (2018) A comprehensive mechanistic model for simulating algal-bacterial growth dynamics in photobioreactors. Bioresour. Technol. 247 (Supplement C) 640-651.

[39] Lucker, B.F., Hall, C.C., Zegarac, R., and Kramer, D.M. (2014) The environmental photobioreactor (ePBR): An algal culturing platform for simulating dynamic natural environments. Algal Res. 6 (Part B) 242-249.

[40] Huesemann, M., Williams, P., Edmundson, S., Chen, P., Kruk, R., Cullinan, V., Crowe, B., and Lundquist, T. (2017) The laboratory environmental algae pond simulator (LEAPS) photobioreactor: Validation using outdoor pond cultures of *Chlorella sorokiniana* and *Nannochloropsis salina*. Algal Res. 26 39-46.

[41] Takolander, A., Leskinen, E., and Cabeza, M. (2017) Synergistic effects of extreme temperature and low salinity on foundational macroalga *Fucus vesiculosus* in the northern Baltic Sea. J. Exp. Mar. Biol. Ecol. 495 (Supplement C) 110-118.

[42] Tsutsui, I., Miyoshi, T., Aue-umneoy, D., Songphatkaew, J., Meeanan, C., Klomkling, S., Sukchai, H., Pinphoo, P., Yamaguchi, I., Ganmanee, M., Maeno, Y., and Hamano, K. (2015) High tolerance of *Chaetomorpha* sp. to salinity and water temperature enables survival and growth in stagnant waters of central Thailand. International Aquatic Research. 7 (1) 47-62.

[43] Singh Khichi, S., Anis, A., and Ghosh, S. (2018) Mathematical modeling of light energy flux balance in flat panel photobioreactor for *Botryococcus braunii* growth, CO_2 biofixation and lipid production under varying light regimes. Biochem. Eng. J. 134 44-56.

[44] Jacob-Lopes, E., Cacia Ferreira Lacerda, L.M., and Franco, T.T. (2008) Biomass production and carbon dioxide fixation by *Aphanothece microscopica Nägeli* in a bubble column photobioreactor. Biochem. Eng. J. 40 (1) 27-34.

[45] Vo, H.-N.-P., Bui, X.-T., Nguyen, T.-T., Nguyen, D.D., Dao, T.-S., Cao, N.-D.-T., and Vo, T.-K.-Q. (2018) Effects of nutrient ratios and carbon dioxide bio-sequestration on biomass growth of *Chlorella* sp. in bubble column photobioreactor. J. Environ. Manage. 219 1-8.

[46] Tamburic, B., Evenhuis, C.R., Crosswell, J.R., and Ralph, P.J. (2018) An empirical process model to predict microalgal carbon fixation rates in photobioreactors. Algal Res. 31 334-346.

[47] Muñoz, R., Alvarez, M.T., Muñoz, A., Terrazas, E., Guieysse, B., and Mattiasson, B. (2006) Sequential removal of heavy metals ions and organic pollutants using an algal-bacterial consortium. Chemosphere. 63 (6) 903-911.

[48] Arun, S., Manikandan, N.A., Pakshirajan, K., Pugazhenthi, G., and Syiem, M.B. (2017) Cu(II) removal by *Nostoc muscorum* and its effect on biomass growth and nitrate uptake: A photobioreactor study. Int. Biodeterior. Biodegrad. 119 111-117.

[49] Richards, R.G. and Mullins, B.J. (2013) Using microalgae for combined lipid production and heavy metal removal from leachate. Ecol Model. 249 59-67.

[50] Cai, T., Park, S.Y., and Li, Y. (2013) Nutrient recovery from wastewater streams by microalgae: Status and prospects. Renew. Sust. Energ. Rev. 19 360-369.

[51] Jung, E.E., Jain, A., Voulis, N., Doud, D.F.R., Angenent, L.T., and Erickson, D. (2014) Stacked optical waveguide photobioreactor for high density algal cultures. Bioresour. Technol. 171 495-499.

[52] Sun, Y., Huang, Y., Liao, Q., Fu, Q., and Zhu, X. (2016) Enhancement of microalgae production by embedding hollow light guides to a flat-plate photobioreactor. Bioresour. Technol. 207 (Supplement C) 31-38.

[53] Guo, X., Yao, L., and Huang, Q. (2015) Aeration and mass transfer optimization in a rectangular airlift loop photobioreactor for the production of microalgae. Bioresour. Technol. 190 189-195.

[54] Shi, J., Podola, B., and Melkonian, M. (2014) Application of a prototype-scale Twin-Layer photobioreactor for effective N and P removal from different process stages of municipal wastewater by immobilized microalgae. Bioresour. Technol. 154 (Supplement C) 260-266.

[55] Ozkan, A., Kinney, K., Katz, L., and Berberoglu, H. (2012) Reduction of water and energy requirement of algae cultivation using an algae biofilm photobioreactor. Bioresour. Technol. 114 542-548.

[56] Sforza, E., Barbera, E., and Bertucco, A. (2015) Improving the photoconversion efficiency: An integrated photovoltaic-photobioreactor system for microalgal cultivation. Algal Res. 10 (Supplement C) 202-209.

[57] Slegers, P.M., Wijffels, R.H., van Straten, G., and van Boxtel, A.J.B. (2011) Design scenarios for flat panel photobioreactors. Appl. Energ. 88 (10) 3342-3353.

[58] de Mooij, T., de Vries, G., Latsos, C., Wijffels, R.H., and Janssen, M. (2016) Impact of light color on photobioreactor productivity. Algal Res. 15 32-42.

[59] Massart, A., Mirisola, A., Lupant, D., Thomas, D., and Hantson, A.-L. (2014) Experimental characterization and numerical simulation of the hydrodynamics in an airlift photobioreactor for microalgae cultures. Algal Res. 6 210-217.

[60] Koller, A.P., Wolf, L., and Weuster-Botz, D. (2017) Reaction engineering analysis of *Scenedesmus ovalternus* in a flat-plate gas-lift photobioreactor. Bioresour. Technol. 225 165-174.

[61] Pfaffinger, C.E., Schöne, D., Trunz, S., Löwe, H., and Weuster-Botz, D. (2016) Model-based optimization of microalgae areal productivity in flat-plate gas-lift photobioreactors. Algal Res. 20 (Supplement C) 153-163.

[62] Boelee, N.C., Janssen, M., Temmink, H., Shrestha, R., Buisman, C.J.N., and Wijffels, R.H. (2014) Nutrient Removal and Biomass Production in an Outdoor Pilot-Scale Phototrophic Biofilm Reactor for Effluent Polishing. Appl. Biochem. Biotechnol. 172 (1) 405-422.

[63] Boelee, N.C., Temmink, H., Janssen, M., Buisman, C.J.N., and Wijffels, R.H. (2011) Nitrogen and phosphorus removal from municipal wastewater effluent using microalgal biofilms. Water Res. 45 (18) 5925-5933.

[64] Martín-Girela, I., Curt, M.D., and Fernández, J. (2017) Flashing light effects on CO_2 absorption by microalgae grown on a biofilm photobioreactor. Algal Res. 25 (Supplement C) 421-430.

[65] Pham, H.-M., Kwak, H.S., Hong, M.-E., Lee, J., Chang, W.S., and Sim, S.J. (2017) Development of an X-Shape airlift photobioreactor for increasing algal biomass and biodiesel production. Bioresour. Technol. 239 211-218.

[66] Janoska, A., Lamers, P.P., Hamhuis, A., van Eimeren, Y., Wijffels, R.H., and Janssen, M. (2017) A liquid foam-bed photobioreactor for microalgae production. Chem. Eng. J. 313 1206-1214.

[67] Hu, J.-Y. and Sato, T. (2017) A photobioreactor for microalgae cultivation with internal illumination considering flashing light effect and optimized light-source arrangement. Energy Convers. Manage. 133 558-565.

[68] Chang, H.-X., Fu, Q., Huang, Y., Xia, A., Liao, Q., Zhu, X., Zheng, Y.-P., and Sun, C.-H. (2016) An annular photobioreactor with ion-exchange-membrane for non-touch microalgae cultivation with wastewater. Bioresour. Technol. 219 668-676.

[69] Eltayeb, A.E., Khalil, O., Al-Hallaj, S., and Teymour, F. (2010) Design and modeling of optical modules for use in the "Emerald Forest" algae photobioreactors. Comput. Chem. Eng. 34 (9) 1323-1340.

[70] Ozkan, A. and Rorrer, G.L. (2017) Effects of light intensity on the selectivity of lipid and chitin nanofiber production during photobioreactor cultivation of the marine diatom *Cyclotella* sp. Algal Res. 25 216-227.

[71] Murray, A.M., Fotidis, I.A., Isenschmid, A., Haxthausen, K.R.A., and Angelidaki, I. (2017) Wirelessly powered submerged-light illuminated photobioreactors for efficient microalgae cultivation. Algal Res. 25 (Supplement C) 244-251.

[72] Pegallapati, A.K., Nirmalakhandan, N., Dungan, B., Holguin, F.O., and Schaub, T. (2014) Evaluation of internally illuminated photobioreactor for improving energy ratio. J. Biosci. Bioeng. 117 (1) 92-98.

[73] López-Rosales, L., García-Camacho, F., Sánchez-Mirón, A., Martín Beato, E., Chisti, Y., and Molina Grima, E. (2016) Pilot-scale bubble column photobioreactor culture of a marine dinoflagellate microalga illuminated with light emission diodes. Bioresour. Technol. 216 845-855.

[74] Serra-Maia, R., Bernard, O., Gonçalves, A., Bensalem, S., and Lopes, F. (2016) Influence of temperature on *Chlorella vulgaris* growth and mortality rates in a photobioreactor. Algal Res. 18 352-359.

[75] Yang, Z., Cheng, J., Yang, W., Zhou, J., and Cen, K. (2016) Developing a water-circulating column photobioreactor for microalgal growth with low energy consumption. Bioresour. Technol. 221 (Supplement C) 492-497.

[76] Cheirsilp, B., Thawechai, T., and Prasertsan, P. (2017) Immobilized oleaginous microalgae for production of lipid and phytoremediation of secondary effluent from palm oil mill in fluidized bed photobioreactor. Bioresour. Technol. 241 787-794.

[77] Ozkan, A. and Rorrer, G.L. (2017) Effects of CO2 delivery on fatty acid and chitin nanofiber production during photobioreactor cultivation of the marine diatom Cyclotella sp. Algal Res.

[78] Tao, Q., Gao, F., Qian, C.-Y., Guo, X.-Z., Zheng, Z., and Yang, Z.-H. (2017) Enhanced biomass/biofuel production and nutrient removal in an algal biofilm airlift photobioreactor. Algal Res. 21 9-15.

[79] Pavlik, D., Zhong, Y., Daiek, C., Liao, W., Morgan, R., Clary, W., and Liu, Y. (2017) Microalgae cultivation for carbon dioxide sequestration and protein production using a high-efficiency photobioreactor system. Algal Res. 25 413-420.

[80] Mohsenpour, S.F. and Willoughby, N. (2013) Luminescent photobioreactor design for improved algal growth and photosynthetic pigment production through spectral conversion of light. Bioresour. Technol. 142 147-153.

[81] Deschênes, J.-S., Boudreau, A., and Tremblay, R. (2015) Mixotrophic production of microalgae in pilot-scale photobioreactors: Practicability and process considerations. Algal Res. 10 80-86.

[82] Cabello, J., Morales, M., and Revah, S. (2014) Dynamic photosynthetic response of the microalga *Scenedesmus obtusiusculus* to light intensity perturbations. Chem. Eng. J. 252 104-111.

[83] Arias, D.M., Uggetti, E., García-Galán, M.J., and García, J. (2017) Cultivation and selection of cyanobacteria in a closed photobioreactor used for secondary effluent and digestate treatment. Sci. Total Environ. 587 157-167.

[84] Lee, C.S., Lee, S.-A., Ko, S.-R., Oh, H.-M., and Ahn, C.-Y. (2015) Effects of photoperiod on nutrient removal, biomass production, and algal-bacterial population dynamics in lab-scale photobioreactors treating municipal wastewater. Water Res. 68 680-691.

[85] Krustok, I., Odlare, M., Truu, J., and Nehrenheim, E. (2016) Inhibition of nitrification in municipal wastewater-treating photobioreactors: Effect on algal growth and nutrient uptake. Bioresour. Technol. 202 238-243.

[86] Zhang, B., Lens, P.N.L., Shi, W., Zhang, R., Zhang, Z., Guo, Y., Bao, X., and Cui, F. (2018) Enhancement of aerobic granulation and nutrient removal by an algal–bacterial consortium in a lab-scale photobioreactor. Chem. Eng. J. 334 2373-2382.

[87] Raeesossadati, M.J., Ahmadzadeh, H., McHenry, M.P., and Moheimani, N.R. (2014) CO_2 bioremediation by microalgae in photobioreactors: Impacts of biomass and CO_2 concentrations, light, and temperature. Algal Res. 6 (Part A) 78-85.

[88] Chen, H.-W., Yang, T.-S., Chen, M.-J., Chang, Y.-C., Lin, C.-Y., Wang, E.I.C., Ho, C.-L., Huang, K.-M., Yu, C.-C., Yang, F.-L., Wu, S.-H., Lu, Y.-C., and Chao, L.K.-P. (2012) Application of power plant flue gas in a photobioreactor to grow *Spirulina* algae, and a bioactivity analysis of the algal water-soluble polysaccharides. Bioresour. Technol. 120 256-263.

[89] Sadeghizadeh, A., Farhad dad, F., Moghaddasi, L., and Rahimi, R. (2017) CO_2 capture from air by *Chlorella vulgaris* microalgae in an airlift photobioreactor. Bioresour. Technol. 243 441-447.

[90] Jacob-Lopes, E., Revah, S., Hernández, S., Shirai, K., and Franco, T.T. (2009) Development of operational strategies to remove carbon dioxide in photobioreactors. Chem. Eng. J. 153 (1) 120-126.

[91] Markou, G., Mitrogiannis, D., Çelekli, A., Bozkurt, H., Georgakakis, D., and Chrysikopoulos, C.V. (2015) Biosorption of Cu_2^+ and Ni_2^+ by *Arthrospira platensis* with different biochemical compositions. Chem. Eng. J. 259 806-813.

[92] Ferreira, L.S., Rodrigues, M.S., de Carvalho, J.C.M., Lodi, A., Finocchio, E., Perego, P., and Converti, A. (2011) Adsorption of Ni_2^+, Zn_2^+ and Pb_2^+ onto dry biomass of *Arthrospira (Spirulina) platensis* and *Chlorella vulgaris*. I. Single metal systems. Chem. Eng. J. 173 (2) 326-333.

[93] Escapa, C., Coimbra, R.N., Paniagua, S., García, A.I., and Otero, M. (2015) Nutrients and pharmaceuticals removal from wastewater by culture and harvesting of *Chlorella sorokiniana*. Bioresour. Technol. 185 276-284.

[94] Ismail, M.M., Essam, T.M., Ragab, Y.M., El-Sayed, A.E.-k.B., and Mourad, F.E. (2017) Remediation of a mixture of analgesics in a stirred-tank photobioreactor using microalgal-bacterial consortium coupled with attempt to valorise the harvested biomass. Bioresour. Technol. 232 364-371.

[95] Escapa, C., Torres, T., Neuparth, T., Coimbra, R.N., García, A.I., Santos, M.M., and Otero, M. (2018) Zebrafish embryo bioassays for a comprehensive evaluation of microalgae efficiency in the removal of diclofenac from water. Sci. Total Environ. 640-641 1024-1033.

[96] Gómez-Pérez, C.A., Espinosa, J., Montenegro Ruiz, L.C., and van Boxtel, A.J.B. (2015) CFD simulation for reduced energy costs in tubular photobioreactors using wall turbulence promoters. Algal Res. 12 1-9.

[97] Henrard, A.A., de Morais, M.G., and Costa, J.A.V. (2011) Vertical tubular photobioreactor for semicontinuous culture of *Cyanobium* sp. Bioresour. Technol. 102 (7) 4897-4900.

[98] Slegers, P.M., van Beveren, P.J.M., Wijffels, R.H., van Straten, G., and van Boxtel, A.J.B. (2013) Scenario analysis of large scale algae production in tubular photobioreactors. Appl. Energ. 105 395-406.

[99] Iluz, D. and Abu-Ghosh, S. (2016) A novel photobioreactor creating fluctuating light from solar energy for a higher light-to-biomass conversion efficiency. Energy Convers. Manage. 126 767-773.

[100] Gómez-Pérez, C.A., Espinosa Oviedo, J.J., Montenegro Ruiz, L.C., and van Boxtel, A.J.B. (2017) Twisted tubular photobioreactor fluid dynamics evaluation for energy consumption minimization. Algal Res. 27 (Supplement C) 65-72.

[101] Concas, A., Malavasi, V., Costelli, C., Fadda, P., Pisu, M., and Cao, G. (2016) Autotrophic growth and lipid production of *Chlorella sorokiniana* in lab batch and BIOCOIL photobioreactors: Experiments and modeling. Bioresour. Technol. 211 327-338.

[102] da Silva, M.F., Casazza, A.A., Ferrari, P.F., Perego, P., Bezerra, R.P., Converti, A., and Porto, A.L.F. (2016) A new bioenergetic and thermodynamic approach to batch

photoautotrophic growth of *Arthrospira (Spirulina) platensis* in different photobioreactors and under different light conditions. Bioresour. Technol. 207 220-228.

[103] Binnal, P. and Babu, P.N. (2017) Statistical optimization of parameters affecting lipid productivity of microalga *Chlorella protothecoides* cultivated in photobioreactor under nitrogen starvation. S. Afr. J. Chem. Eng. 23 26-37.

[104] Vitova, M., Bisova, K., Kawano, S., and Zachleder, V. (2015) Accumulation of energy reserves in algae: From cell cycles to biotechnological applications. Biotechnol. Adv. 33 (6, Part 2) 1204-1218.

[105] Zhang, W., Zhao, Y., Cui, B., Wang, H., and Liu, T. (2016) Evaluation of filamentous green algae as feedstocks for biofuel production. Bioresour. Technol. 220 407-413.

[106] Saeid, A. and Chojnacka, K. (2015) Toward production of microalgae in photobioreactors under temperate climate. Chem. Eng. Res. Des. 93 377-391.

[107] Kang, D., Zhao, Q., Wu, Y., Wu, C., and Xiang, W. (2017) Removal of nutrients and pharmaceuticals and personal care products from wastewater using periphyton photobioreactors. Bioresour. Technol.

[108] Hamano, H., Nakamura, S., Hayakawa, J., Miyashita, H., and Harayama, S. (2017) Biofilm-based photobioreactor absorbing water and nutrients by capillary action. Bioresour. Technol. 223 307-311.

[109] Hom-Diaz, A., Jaén-Gil, A., Bello-Laserna, I., Rodríguez-Mozaz, S., Vicent, T., Barceló, D., and Blánquez, P. (2017) Performance of a microalgal photobioreactor treating toilet wastewater: Pharmaceutically active compound removal and biomass harvesting. Sci. Total Environ. 592 1-11.

[110] García-Galán, M.J., Gutiérrez, R., Uggetti, E., Matamoros, V., García, J., and Ferrer, I. (2018) Use of full-scale hybrid horizontal tubular photobioreactors to process agricultural runoff. Biosys. Eng. 166 138-149.

[111] Jones, S.M.J., Louw, T.M., and Harrison, S.T.L. (2017) Energy consumption due to mixing and mass transfer in a wave photobioreactor. Algal Res. 24 317-324.

[112] Schreiber, C., Behrendt, D., Huber, G., Pfaff, C., Widzgowski, J., Ackermann, B., Müller, A., Zachleder, V., Moudříková, Š., Mojzeš, P., Schurr, U., Grobbelaar, J., and Nedbal, L. (2017) Growth of algal biomass in laboratory and in large-scale algal photobioreactors in the temperate climate of western Germany. Bioresour. Technol. 234 140-149.

[113] Parladé, E., Hom-Diaz, A., Blánquez, P., Martínez-Alonso, M., Vicent, T., and Gaju, N. (2018) Effect of cultivation conditions on β-estradiol removal in laboratory and pilot-plant photobioreactors by an algal-bacterial consortium treating urban wastewater. Water Res. 137 86-96.

[114] de Jesus, S.S. and Maciel Filho, R. (2017) Potential of algal biofuel production in a hybrid photobioreactor. Chem. Eng. Sci. 171 (Supplement C) 282-292.

[115] Xu, X.-Q., Wang, J.-H., Zhang, T.-Y., Dao, G.-H., Wu, G.-X., and Hu, H.-Y. (2017) Attached microalgae cultivation and nutrients removal in a novel capillary-driven photo-biofilm reactor. Algal Res. 27 198-205.

[116] Pruvost, J., Le Borgne, F., Artu, A., and Legrand, J. (2017) Development of a thin-film solar photobioreactor with high biomass volumetric productivity (AlgoFilm©) based on process intensification principles. Algal Res. 21 120-137.

[117] Fu, Q., Li, Y., Zhong, N., Liao, Q., Huang, Y., Xia, A., Zhu, X., and Hou, Y. (2017) A novel biofilm photobioreactor using light guide plate enhances the hydrogen production. Int. J. Hydrogen Energy. 42 (45) 27523-27531.

[118] Gao, F., Yang, Z.-H., Li, C., Zeng, G.-M., Ma, D.-H., and Zhou, L. (2015) A novel algal biofilm membrane photobioreactor for attached microalgae growth and nutrients removal from secondary effluent. Bioresour. Technol. 179 8-12.

[119] Gao, F., Li, C., Yang, Z.-H., Zeng, G.-M., Feng, L.-J., Liu, J.-z., Liu, M., and Cai, H.-w. (2016) Continuous microalgae cultivation in aquaculture wastewater by a membrane photobioreactor for biomass production and nutrients removal. Ecol. Eng. 92 55-61.

[120] Praveen, P., Heng, J.Y.P., and Loh, K.-C. (2016) Tertiary wastewater treatment in membrane photobioreactor using microalgae: Comparison of forward osmosis & microfiltration. Bioresour. Technol. 222 448-457.

[121] Sun, L., Tian, Y., Zhang, J., Li, H., Tang, C., and Li, J. (2018) Wastewater treatment and membrane fouling with algal-activated sludge culture in a novel membrane bioreactor: Influence of inoculation ratios. Chem. Eng. J. 343 455-459.

[122] Yang, J., Gou, Y., Fang, F., Guo, J., Lu, L., Zhou, Y., and Ma, H. (2018) Potential of wastewater treatment using a concentrated and suspended algal-bacterial consortium in a photo membrane bioreactor. Chem. Eng. J. 335 154-160.

[123] Low, S.L., Ong, S.L., and Ng, H.Y. (2016) Characterization of membrane fouling in submerged ceramic membrane photobioreactors fed with effluent from membrane bioreactors. Chem. Eng. J. 290 91-102.

[124] Sun, L., Tian, Y., Zhang, J., Cui, H., Zuo, W., and Li, J. (2018) A novel symbiotic system combining algae and sludge membrane bioreactor technology for wastewater treatment and membrane fouling mitigation: Performance and mechanism. Chem. Eng. J. 344 246-253.

[125] Viruela, A., Robles, Á., Durán, F., Ruano, M.V., Barat, R., Ferrer, J., and Seco, A. (2018) Performance of an outdoor membrane photobioreactor for resource recovery from anaerobically treated sewage. J. Cleaner Prod. 178 665-674.

[126] Bilad, M.R., Discart, V., Vandamme, D., Foubert, I., Muylaert, K., and Vankelecom, I.F.J. (2014) Coupled cultivation and pre-harvesting of microalgae in a membrane photobioreactor (MPBR). Bioresour. Technol. 155 410-417.

[127] Fuentes-Grünewald, C., Bayliss, C., Fonlut, F., and Chapuli, E. (2016) Long-term dinoflagellate culture performance in a commercial photobioreactor: *Amphidinium carterae* case. Bioresour. Technol. 218 533-540.

[128] Gao, F., Peng, Y.-Y., Li, C., Cui, W., Yang, Z.-H., and Zeng, G.-M. (2018) Coupled nutrient removal from secondary effluent and algal biomass production in membrane photobioreactor (MPBR): Effect of HRT and long-term operation. Chem. Eng. J. 335 169-175.

[129] Fu, Q., Chang, H.-X., Huang, Y., Liao, Q., Zhu, X., Xia, A., and Sun, Y.-H. (2016) A novel self-adaptive microalgae photobioreactor using anion exchange membranes for continuous supply of nutrients. Bioresour. Technol. 214 629-636.

[130] Najm, Y., Jeong, S., and Leiknes, T. (2017) Nutrient utilization and oxygen production by *Chlorella vulgaris* in a hybrid membrane bioreactor and algal membrane photobioreactor system. Bioresour. Technol. 237 64-71.

[131] Podevin, M., Fotidis, I.A., De Francisci, D., Møller, P., and Angelidaki, I. (2017) Detailing the start-up and microalgal growth performance of a full-scale photobioreactor operated with bioindustrial wastewater. Algal Res. 25 101-108.

[132] Lee, Y.-S. and Han, G.-B. (2016) Complete reduction of highly concentrated contaminants in piggery waste by a novel process scheme with an algal-bacterial symbiotic photobioreactor. J. Environ. Manage. 177 202-212.

[133] Maza-Márquez, P., González-Martínez, A., Rodelas, B., and González-López, J. (2017) Full-scale photobioreactor for biotreatment of olive washing water: Structure and diversity of the microalgae-bacteria consortium. Bioresour. Technol. 238 389-398.

[134] Binnal, P. and Babu, P.N. (2017) Optimization of environmental factors affecting tertiary treatment of municipal wastewater by Chlorella protothecoides in a lab scale photobioreactor. J. Water Proc. Eng. 17 290-298.

[135] Marbelia, L., Bilad, M.R., Passaris, I., Discart, V., Vandamme, D., Beuckels, A., Muylaert, K., and Vankelecom, I.F.J. (2014) Membrane photobioreactors for integrated microalgae cultivation and nutrient remediation of membrane bioreactors effluent. Bioresour. Technol. 163 228-235.

[136] Taleb, A., Kandilian, R., Touchard, R., Montalescot, V., Rinaldi, T., Taha, S., Takache, H., Marchal, L., Legrand, J., and Pruvost, J. (2016) Screening of freshwater and seawater microalgae strains in fully controlled photobioreactors for biodiesel production. Bioresour. Technol. 218 (Supplement C) 480-490.

[137] Solimeno, A., Acíen, F.G., and García, J. (2017) Mechanistic model for design, analysis, operation and control of microalgae cultures: Calibration and application to tubular photobioreactors. Algal Res. 21 (Supplement C) 236-246.

[138] Hou, Q., Nie, C., Pei, H., Hu, W., Jiang, L., and Yang, Z. (2016) The effect of algae species on the bioelectricity and biodiesel generation through open-air cathode microbial fuel cell with kitchen waste anaerobically digested effluent as substrate. Bioresour. Technol. 218 902-908.

[139] Ge, S. and Champagne, P. (2017) Cultivation of the Marine Macroalgae *Chaetomorpha linum* in Municipal Wastewater for Nutrient Recovery and Biomass Production. Environ. Sci. Technol. 51 (6) 3558-3566.

[140] Zhu, L., Wang, Z., Shu, Q., Takala, J., Hiltunen, E., Feng, P., and Yuan, Z. (2013) Nutrient removal and biodiesel production by integration of freshwater algae cultivation with piggery wastewater treatment. Water Res. 47 (13) 4294-4302.

[141] Pruvost, J., Le Gouic, B., Lepine, O., Legrand, J., and Le Borgne, F. (2016) Microalgae culture in building-integrated photobioreactors: Biomass production modelling and energetic analysis. Chem. Eng. J. 284 850-861.

[142] Dutt, F., Quan, S.J., Woodworth, E., Castro-Lacouture, D., Stuart, B.J., and Yang, P.P.-J. (2017) Modeling algae powered neighborhood through GIS and BIM integration. Energy Procedia. 105 3830-3836.

[143] Zijffers, J.-W.F., Salim, S., Janssen, M., Tramper, J., and Wijffels, R.H. (2008) Capturing sunlight into a photobioreactor: Ray tracing simulations of the propagation of light from capture to distribution into the reactor. Chem. Eng. J. 145 (2) 316-327.

[144] Barbera, E., Sforza, E., Guidobaldi, A., Di Carlo, A., and Bertucco, A. (2017) Integration of dye-sensitized solar cells (DSC) on photobioreactors for improved photoconversion efficiency in microalgal cultivation. Renew. Energ. 109 13-21.

[145] Ruiz, J., Olivieri, G., de Vree, J., Bosma, R., Willems, P., Reith, J.H., Eppink, M.H.M., Kleinegris, D.M.M., Wijffels, R.H., and Barbosa, M.J. (2016) Towards industrial products from microalgae. Energy Environ. Sci. 9 (10) 3036-3043.

[146] Judd, S.J., Al Momani, F.A.O., Znad, H., and Al Ketife, A.M.D. (2017) The cost benefit of algal technology for combined CO_2 mitigation and nutrient abatement. Renew. Sust. Energ. Rev. 71 379-387.

[147] Pruvost, J., Le Borgne, F., Artu, A., Cornet, J.-F., and Legrand, J., Chapter Five - Industrial Photobioreactors and Scale-Up Concepts, in *Advances in Chemical Engineering*, Legrand, J., Editor. 2016, Academic Press. p. 257-310.

[148] Öncel, S.Ş., Köse, A., and Öncel, D.Ş., 11 - Façade integrated photobioreactors for building energy efficiency, in *Start-Up Creation*. 2016, Woodhead Publishing. p. 237-299.

[149] Algae Competition, The 2011 International Algae Competition (2018) Available from: http://www.algaecompetition.com/algae-slideshows/algae-architecture/ (accessed 10 April 2018).

[150] Issarapayup, K., Powtongsook, S., and Pavasant, P. (2011) Economical review of Haematococcus pluvialis culture in flat-panel airlift photobioreactors. Aquacult. Eng. 44 (3) 65-71.

[151] Huang, J., Ying, J., Fan, F., Yang, Q., Wang, J., and Li, Y. (2016) Development of a novel multi-column airlift photobioreactor with easy scalability by means of computational fluid dynamics simulations and experiments. Bioresour. Technol. 222 399-407.

[152] Koller, M., Design of Closed Photobioreactors for Algal Cultivation, in *Algal Biorefineries: Volume 2: Products and Refinery Design*, Prokop, A., Bajpai, R.K., and Zappi, M.E., Editors. 2015, Springer International Publishing: Cham. p. 133-186.

[153] AlgaSol Renewable, Technology (2018) Available from: http://www.algasolrenewables.com/index.php/price-list (accessed 9 August 2018).

[154] Jay, A.R., Algal Bioenergy Program (2013) Available from: http://newscenter.nmsu.edu/Articles/view/9281/power-nmsu-explores-algal-biofuel-production-from-wastewater (accessed 9 August 2018).

[List of tables]

Table 1. Algae growth dynamic models.

Eq. No.	Model name	Model Equations	References
Eq. 1	Monod model	$\frac{dX}{dt} = \bar{\mu} * X$	Lee et al. [22]
Eq. 2	Modified Monod model	$\frac{dX}{dt} = (\mu_X - K_d) * X$	Al Ketife et al. [15]
Eq. 3	Droop model	$\frac{dX}{dt} = (1 - \frac{k_q}{q}) * \frac{I}{I + k_s} * \left[A * e^{-\frac{E_a}{R*T}} - B * e^{-\frac{E_b}{R*T}}\right] * X - \mu_d * X^2$	Zhang et al. [16]
Eq. 4	Luedeking-Piret model	$\frac{dX}{dt} = \left(1 - \frac{k_q}{q}\right) * \frac{k_q}{q} * \frac{I}{I + k_s} * \left[A * e^{-\frac{E_a}{R*T}} - B * e^{-\frac{E_b}{R*T}}\right] * X - \mu_d * X^2$	
Eq . 5	Biofilm thickness (self-derived model)	$\frac{d(Th)}{dt} = p \times \frac{dX}{dt}$	Das et al. [23]
Eq. 6	Modified Droop model	$X_i \frac{dP_i}{dt} = X_i\big(\rho(S_i, P_i) - (P_i + P_{min})\mu_X(P_i, I_i)\big) + \frac{QX_{i-1}}{V_i}(P_{i-1} - P_i)$	Diehl et al. [24]
Eq. 7	Modified Monod model	$\frac{dX}{dt} = \bar{\mu} * X * b^T$	Ye et al. [26]

Table 2. The dynamic models of C, N, P assimilation in PBs

Eq. No.	Components	Model Equations	References
Eq. 8	TC Assimilation Rate	$\frac{d[TC]}{dt} = \frac{d[AC]}{dt} + \frac{d[DIC]}{dt} + \frac{d[DOC]}{dt}$	
Eq. 9	TN Assimilation Rate	$\frac{d[TN]}{dt} = \frac{d[AN]}{dt} + \frac{d[DIN]}{dt}$	Shriwastav et al. [21] Shriwastav et al. [38]
Eq. 10	TP Assimilation Rate	$\frac{d[TP]}{dt} = \frac{d[AP]}{dt} + \frac{d[DIP]}{dt}$	
Eq. 11	C Uptake Rate	$\frac{dC}{dt} = -1000 Y_C \mu_X X$	Al Ketife et al. [15]
Eq. 12	N and P Balance	$\frac{dC_{N,P}}{dt} = -1000 Y_{N,P} \mu_X X$	

Eq. 13	CO_2 Uptake Rate	$R_{CO2} = C_c \times \mu_L \times \frac{M_{CO2}}{M_C}$	Singh Khichi et al. [43] Vo et al. [45] Jacob-Lopes et al. [44]
Eq. 14	C Fixation rate	$\frac{dC}{dt} = P_{HCO3} \frac{[HCO_3^-]}{[HCO_3^-] + K_{HCO_3^-}}^{-R_1}{}_{-R_3} + P_{CO_2} \frac{[CO_2]}{[CO_2] + K_{CO_2}}$	Tamburic et al. [46]
Eq. 14	Fe Uptake Rate	$v_{Fe} = v_{Fe}^{max}(\frac{Q_{Fe}^{max} - q_{Fe}}{Q_{Fe}^{max} - Q_{Fe}^{min}}) \frac{C_{Fe(III)}}{K_{Fe} + C_{Fe(III)}}$	Concas et al. [27]
Eq. 15	Adsorbed Metal Complex for Microalgae i	$\frac{d[MetalALG_{ij}]}{dt} = adsorb_{Me-ALG,ji}$	Richards and Mullins [49]
Eq. 16	Adsorption of Metal j to Microalgae i	$Adsorb_{Me,ALGji} = Metal_{F,j} \times AR_j \times \frac{ALG_i}{\sum ALG}$	
Eq. 17	Modified Han-Levenspiel	$r = r_{max}\left(1 - \frac{C}{C_{cri}}\right)^m$	Arun et al. [48]

Eq. 18	Non-competitive inhibition	$r = \frac{r_{max} K_c}{K_C + C}$

Eq. 19	Andrews	$r = \frac{r_{max} K_c}{K_s + C + \frac{C^2}{k_i}}$

Table 3. Main advantages and disadvantages of tubular, column, and flat plate and hybrid PBs.

PB types	Advantages	Disadvantages	
Flat plate PBs	Large illumination surface area	Require space and land availability	Yadala and Cremaschi [11] Posten and Walter [1] Jung et al. [51] de Mooij et al. [58] Ozkan et al. [55]
	Suitable for outdoor cultivation	Has photoinhibition effect	
	High biomass yield	Dark zone formation	
	Modular configuration	High construction and energy costs	
	Preferable in PB-based architecture		
Column PBs	High mass transfer	Moderate illumination area, prefers inner illumination	Mirón et al. [13] Yadala and Cremaschi [11] López et al. [12] Posten and Walter [1]
	Sufficient mixing	Low surface to volume ratio	
	Compact and easy to operate	High mixing cost	
	Greater gas hold ups	Illumination surface reduce while scaling up	
	Best exposure to light/dark cycles		

	Easy to scale up		
	Minor fouling problem		
Tubular PBs	Large illumination surface area	Requires a number of modules to increase scale	Slegers et al. [98] Posten and Walter [1] Saeid and Chojnacka [106] Yadala and Cremaschi [11] López et al. [12]
	Easy to construct, maintain, and clean	Fouling	
	High mass transfer	Over-heating	
	Low power consumption	Expensive to operate	
Soft-frame PBs	Flexible	Easily damaged materials	Hamano et al. [108] Hom-Diaz et al. [109]
	Foldable	Insufficient mixing due to dead zone formation	
	Replaceable	Culture leakage	
	Less space required	Expensive material costs	
Hybrid PBs	Reduce reactor size	Membrane fouling	Sheng et al. [10] Marbelia et al. [135]
	Operate with higher dilution rate		
	Biomass with higher carbohydrate and	Negative energy balance	

	lower protein content		
	Minimize washout problem		
	Low O&M cost		

Table 4. Performance of types of PBs in certain operating conditions.

No.	Configuration	Type of PB	Algae species	Light irradiance (μmol/$m^2.s^1$)	Light-dark cycle (h:h)	Light source	Biomass concentration (g/L)	Biomass productivity	References
1	Flat plate in PBs	Flat plate	*Botryococcus braunii*	100	24:0	Fluorescent	96.4	0.71 g/m^2	Ozkan et al. [55]
2	Flat plate gas-lift PBs	Flat plate	*Scenedesmus ovalternus*	1300	24:0	LED	7.5	0.11/d 25.0 ± 0.5 $g/m^2.d$	Koller et al. [60]
3	Flat-panel airlift PBs	Flat plate	*Chlamydomonas reinhardtii*	1500	24:0	LED	4.5	29 - 54 $g/m^2.d$	de Mooij et al. [58]

4	Foam-bed PBs	Column	*Chlorella sorokiniana*	334 ± 16	n.d	LED	4.7	0.10/h	Janoska et al. [66]
5	Closed PBs	Column	Green algae (genus *Chlorella* and *Stigeoclonium*) and cyanobacteria (cf. *Oscillatoria*)	204	12:12	Metal halide	0.49 - 0.84	0.039-0.084 g/L.d	Arias et al. [83]
6	X-Shape PBs	Column	*Chlamydomonas reinhardti*	100	11:13	LED	1.359 ± 0.007	-	Pham et al. [65]
7	Water-circulating column PBs	Column	*Chlorella* mutant *PY-ZU1*	40 ± 2 klx	24:0	n.d	n.d	112.6 mg/L.d	Yang et al. [75]

8	Vertical multi-column airlift PBs	Column	*Chlorella pyrenoidosa*	672	n.d	Solar light	1.3-1.56	n.d	Huang et al. [151]
9	Internal illumination PBs	Column	*Dunaliella tertiolecta*	250, 420 and 1000	Continuous or flash	LED	19.78	10.18 g/L.d	Hu and Sato [67]
10	Ion-exchange membrane PBs	Column	*Chlorella vulgaris*	110	n.d	Fluorescent	4.24, 3.13 and 2.04	0.30 ± 0.04, 0.23 ± 0.01 and 0.17 ± 0.01 g/L.d	Chang et al. [68]
11	BIOCOIL PBs	Tubular	*Chlorella sorokiniana*	100	12:12	White fluorescent	0.9 - 1	0.52/d	Concas et al. [101]
12	Horizontal PBs	Tubular	*Arthrospira platensis*	70	n.d	Fluorescent	7.11 ± 0.53	0.86 ± 0.03 g/L.d	da Silva et al. [102]

13	Horizontal and vertical tubular PBs	Tubular	*Phaeodactylum tricornutum* *Thalassiosira pseudonana*	50-700 W/m^2	Natural light cycle	Sunlight	0.2 - 12	1.4 - 3.29/d	Slegers et al. [98]
14	Combined-light PBs	Tubular	*Nannochloropsis salina*	500	24:0	LED	7.2	0.888/d	Iluz and Abu-Ghosh [99]
15	Macroalgae PBs	Soft-frame	*Cladophora* sp., *Ulva compressa* and *Ulva rigida*	238 - 348	Varied	Solar	n.d	n.d	Chemodanov et al. [8]
16	Biofilm-based PBs	Soft-frame	*Pseudochoricystis ellipsoidea*	300 - 340	12:12 and 24:0	LED	n.d	8 –10 g/m^2.d	Hamano et al. [108]

17	Environmental PBs	Others	*Chlorella sorokiniana* and *Chlamydomonas reinhardtii*	2500	12:12 and 14:10	LED	2.5 - 15	19.1 - 19.7 $g/m^2.d$	Lucker et al. [39]
18	Capillary-driven PBs	Hybrid	*Scenedesmus* sp. LX1	144	14:10	n.d	n.d	10 $g/m^2.d$	Xu et al. [115]
19	Membrane PBs	Hybrid	*Chlorella vulgaris*	n.d	n.d	n.d	2.03	4.47-8.25 g/d	Bilad et al. [126]
20	Floating horizontal PBs	Hybrid	*Nannochloris atomus* Butcher CCAP 251/4A	n.d	n.d	Outdoor condition	2.07 - 4.3	18.2 $g\ m^{-2}\ d^{-1}$	Dogaris et al. [14]

n.d: no data

Table 5. The removal of contaminants by PBs

No.	Configuration	Type of PB	Waste water source	Algae species	Removal efficiency (%)					References
					TN	TP	COD	PPCPs & organic	Others	
1	Twin-layer PBs	Flat plate	Municipal wastewater	*Halochlorella rubescens*	70-99		n.d	n.d	n.d	Shi et al. [54]
2	Plastic sheet PBs	Flat plate	Municipal wastewater	Various	Uptake 1.0 g/m^2.d	Uptake 0.13 g/m^2.d	n.d	n.d	n.d	Boelee et al. [63]
3	Lab scale PBs	Column	Synthetic wastewater	Algae and bacteria consortium	60.4 – 70.5	93.2 – 96.4	95.5 - 96.7	n.d	n.d	Zhang et al. [86]
4	Batch PBs	Column	Municipal wastewater after	*Coelastrum micropor um*	35 - 88	43 - 89	59 - 80	n.d	n.d	Lee et al. [84]

			anaerobic digestion							
5	Air-lift PBs	Column	Bio-industrial wastewater	*Chlorella sorokiniana*	100	100	86.84	n.d	n.d	Podevin et al. [131]
6	Bubble Column PBs	Column	Synthetic wastewater	*C. vulgaris*	60 - 99	100	n.d	n.d	n.d	Al Ketife et al. [15]
7	Full scale Tubular PBs	Tubular	Olive washing water	*Sphaeropleales*	n.d	n.d	85.86 ± 1.24	94.84 ± 0.55	n.d	Maza-Márquez et al. [133]
8	Lab scale tubular PBs	Tubular	Artificial wastewater and CO_2 gas	*Chlorella prototheca oides*	n.d	n.d	n.d	n.d	273.66 mg/L.d (CO_2 fixat	Binnal and Babu [103]

									ion rate)	
9	Multi-tubular PBs	Soft-frame	Toilet wastewater	*Trametes versicolor*	80	80	80	98% anti-inflammatory drugs 48% antibiotics 30-57% psychiatric drugs	n.d	Hom-Diaz et al. [109]
10	Multi-tubular PBs	Soft-frame	Urban wastewater	*Scenedesmus* sp. and microbial consortium	n.d	n.d	n.d	100% 17β-estradiol	n.d	Parladé et al. [113]
11	Full scale horizontal	Soft-frame	Agricultural run-off	*Pediastrum* sp., *Chlorella* sp., *Scenedes*	n.d	n.d	n.d	73% tonalide 68% galaxolide	n.d	García-Galán et al. [110]

	tubular PBs			*mus* sp., and the cyanobacteria *Gloeothece* sp				61% anti-inflammatory compounds		
12	Lab scale PBs	Hybrid	Municipal wastewater	*Chlorella prototheca oides*	100	100	78.03	n.d	n.d	Binnal and Babu [134]
13	Microfiltration Membrane PBs	Hybrid	Tertiary wastewater	*C. vulgaris*	86 - 99	100	n.d	n.d	n.d	Praveen et al. [120]
14	Forward Osmosis Membrane PBs				48 - 97	46	n.d	n.d	n.d	
15	Membrane PBs	Hybrid	Synthetic wastewater	*C. vulgaris*	11.6 - 24.5	100	100 (inorganic carbon)	n.d	n.d	Najm et al. [130]

16	Membrane PBs	Hybrid	Aquaculture wastewater	*C. vulgaris* *Scenedesmus obliquus*	86.1	82.7	n.d	n.d	n.d	Gao et al. [119]
17	Periphyton PBs	Others	Surface water	Various	39 - 77	15.8 - 68	n.d	6.45 - 86.4	n.d	Kang et al. [107]
18	Batch PBs	Others	Metal polluted wastewater	*Nostoc muscorum*	n.d	n.d	n.d	n.d	100 (Cu)	Arun et al. [48]

n.d: no data

Table 6. Key characteristics of photobioreactors' integration into building façade (adapted from Öncel et al. [148])

Components	Criteria	Applications
Materials	Durable Cost competitive Lightweight	Prefer high-wind-speed and physical shock resistant materials
Illumination	Sunlight as main illumination source	Applied photochromic glasses or electronically tinting glass films Design proper orientation capability and modular units Using special light collectors, such as Green Solar Collector or Dye-sensitized Solar Cells
Temperature	Adapt to the fluctuation of outdoor condition	Integrated thermal controllers and ventilation systems to optimize temperature
Water	Considering the reuse of building's wastewater for algae cultivation	Wastewater such as domestic wastewater, rain water
Air	Employed the CO_2 exhaust of building	Feeding air by energy-saving systems Monitoring air quality

		Circle air flow in case of high inlet CO_2 concentration Design PBs exhaust valve to release CO_2 of algae's respiration in night time
Biomass and valuable products	Biomass offered valuable income to cut off building's expenditures	Construct sewage-like piping system to process biomass in a central plant which saving transportation and labour costs. Support a sustainable algae market.
Culture maintenance	Notice on the harvesting, contamination prevention, and control	Assign a responsible centre/division

Table 7. Cost analysis of PBs based on the scale factors and functions [5]

PBs cost – Closed vertical type		PBs area (m^2)				
		100	200	500	1000	5000
Bio-Fertilizer and Irrigation	Total cost (€)	6695.5	8535.9	11296.4	15897.3	52704.5
	Cost per m^2 (€)	67	42.7	22.6	15.9	10.5
Heat Generation	Total cost (€)	9060.5	11373.9	14843.9	20627.3	66894.5
	Cost per m^2 (€)	90.6	56.9	29.7	20.6	13.4
Electricity and Heat Generation	Total cost (€)	10060.5	12573.9	16343.9	22627.3	77894.5
	Cost per m^2 (€)	100.6	62.9	32.7	22.6	15.6

[List of Figures]

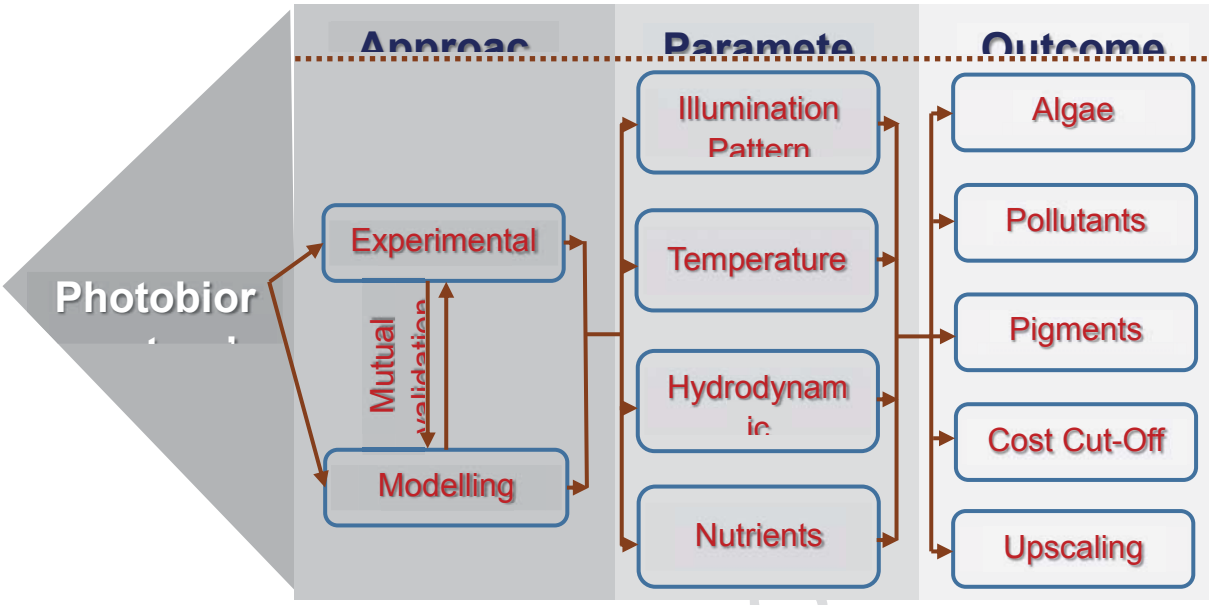

Figure 1. Conceptual framework of PBs design.

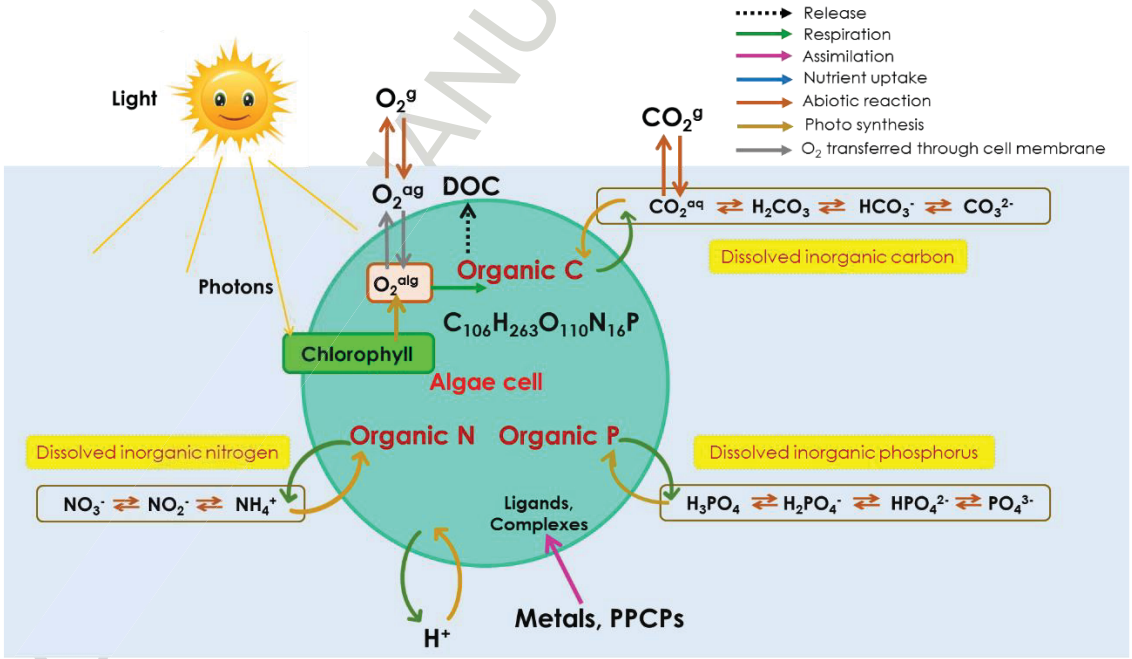

Figure 2. The details of biochemical processes in microalgae-based PBs

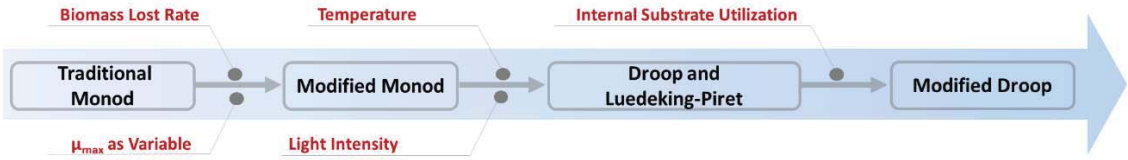

Figure 3. The development of biomass growth models.

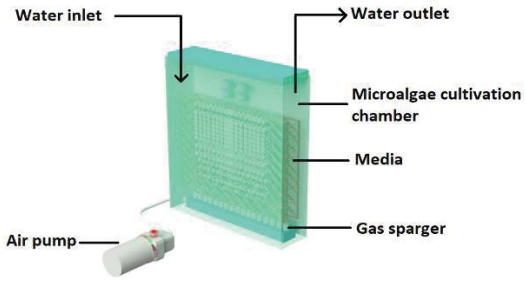

(a)

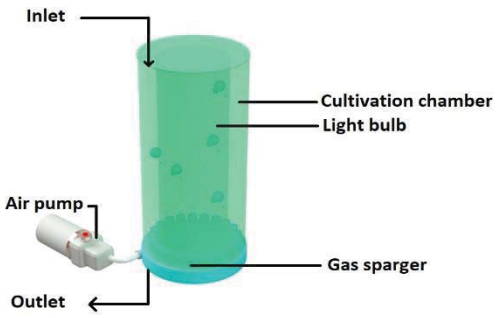

(b)

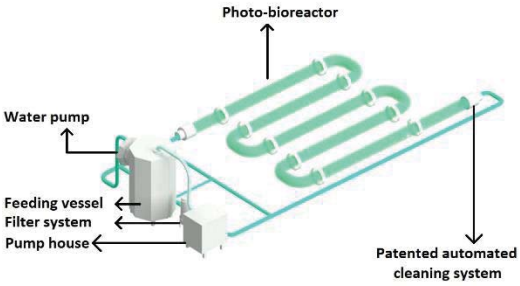

(c)

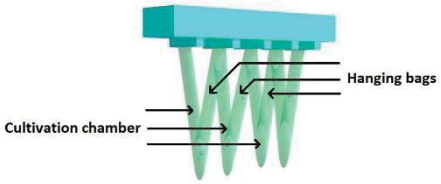

(d)

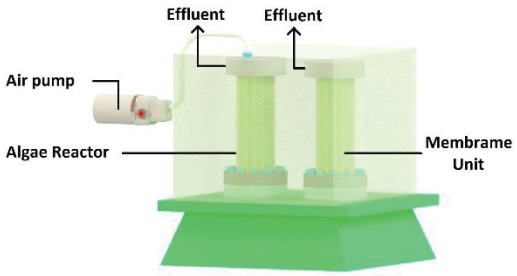

(e)

Figure 4. Common types of PBs (a) Flat plate, (b) Column, (c) Tubular, (d) Soft-frame and (e) Hybrid PBs

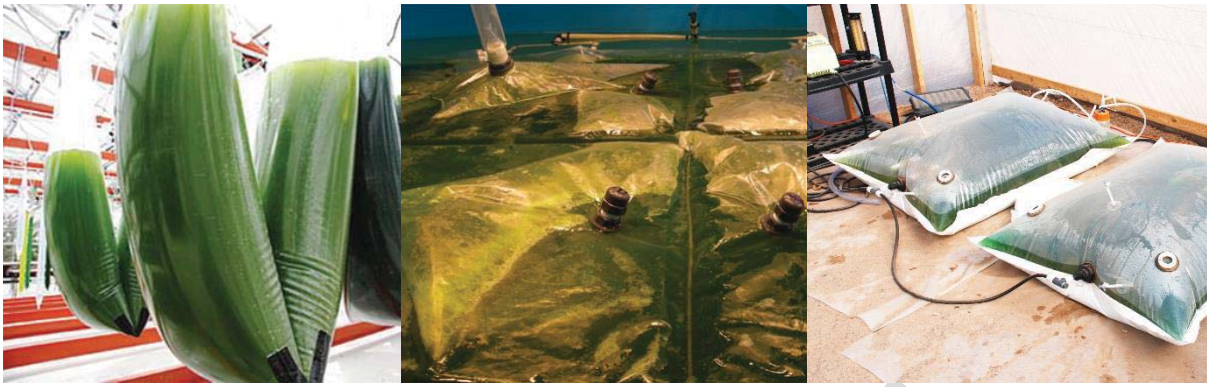

Figure 5. Modified configurations of soft-frame PBs (a) Hanging [152], (b) Floating [153] and (c) Ground-lying [154]

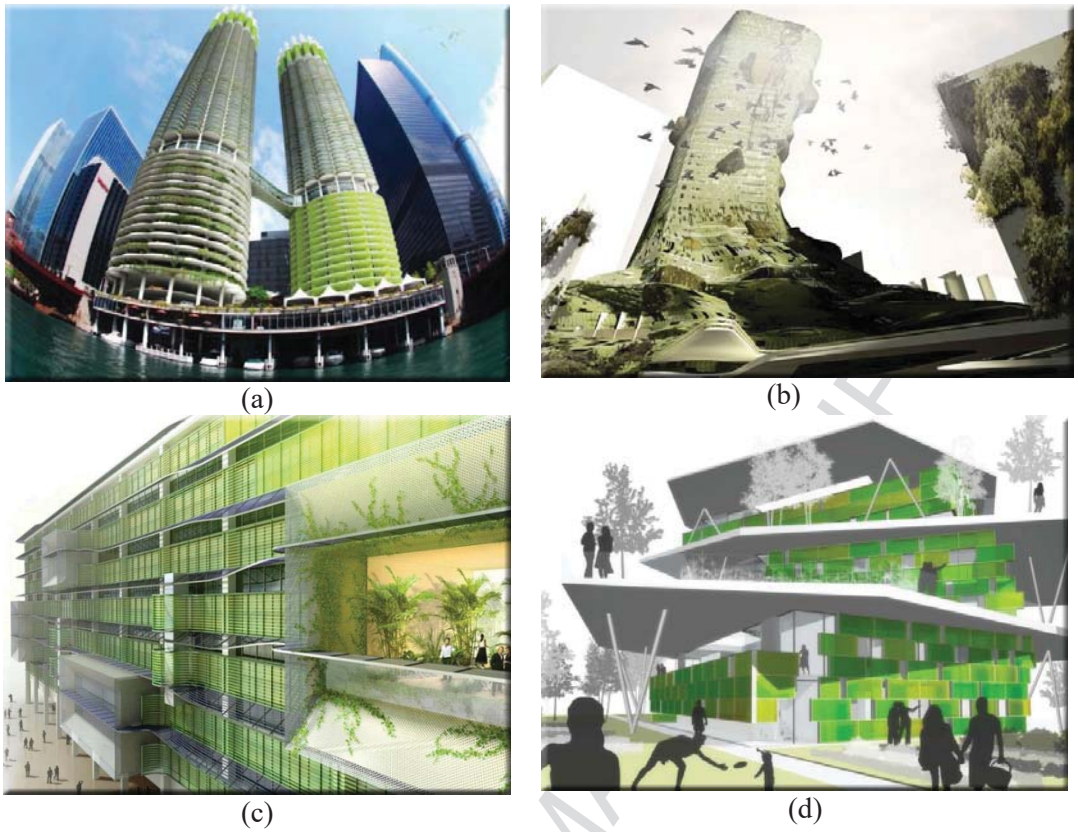

(a) (b)

(c) (d)

Figure 6. The future development of algae-based architecture and infrastructure. (a) Green Loop: Marina City Global Algae Retrofitting, Chicago. (b) Ecologies of Biodiversity: A Self Sustaining Tower for London. (c) Process Zero: Retrofit Resolution. GSA Federal Building, Los Angeles, CA. (d) Hydral Housing units with modular hydrogen producing panels [149]